Nuclear Fuel Behaviour under RIA Conditions

Authors

Peter Rudling
ANT International

Lars Olof Jernkvist
Quantum Technologies AB

With technical contributions from

Friedrich Garzarolli

Ron Adamson

Tahir Mahmood

Alfred Strasser

Charles Patterson

A.N.T. INTERNATIONAL®

Advanced Nuclear Technology International
Analysvägen 5, SE-435 33 Mölnlycke
Sweden

info@antinternational.com
www.antinternational.com


Ecolabelled printed matter, 441 799

Disclaimer

The information presented in this report has been compiled and analysed by Advanced Nuclear Technology International Europe AB (ANT International®) and its subcontractors. ANT International has exercised due diligence in this work, but does not warrant the accuracy or completeness of the information. ANT International does not assume any responsibility for any consequences as a result of the use of the information for any party, except a warranty for reasonable technical skill, which is limited to the amount paid for this assignment by each Project programme member.

Contents

1 Introduction

A reactivity initiated accident (RIA) is a nuclear reactor accident that involves an unwanted increase in fission rate and reactor power. Possible accident scenarios in light water reactors (LWRs) include reactor control system failures and control element ejections, but also events caused by inadvertent changes to the reactor coolant, leading to improved neutron moderation [International Atomic Energy Agency (IAEA), 1993]. The power increase may damage the fuel and reactor core, and in severe cases, create pressure pulses in the reactor coolant. The main safety concern is that the generation of a coolant pressure pulse could break the reactor coolant pressure boundary or damage the fuel and other core internals so that long-term cooling of the core would be impaired. To preclude this, some scenarios for reactivity initiated accidents have been identified by regulatory bodies as design basis accidents, i.e. they are classified as accidents that a reactor must be designed and built to withstand.

In current pressurized water reactors (PWRs) and boiling water reactors (BWRs), which are the two most common types of power generating reactors worldwide [Bodansky, 2004], protection against reactivity initiated accidents is afforded by engineered safety systems, but also by inherent reactor feedback mechanism. More precisely, the reactors are designed so that an unwanted power rise produces fast negative reactivity feedback through the increase in fuel and coolant temperature, and also by steam generation in the light water coolant. The negative feedback limits the peak power and provides time for the engineered safety systems to respond and shut the reactor down. No reactivity initiated accident with severe consequences has so far occurred with the PWR and BWR reactor designs.

1.1 Historical background to reactivity initiated accidents and research

The first reactivity initiated accidents occurred in the 1950s and 1960s and concerned the first generation of research reactors [McLaughlin et al, 2000]. Examples are the 1952 accident in the NRX reactor at Chalk River, Canada [Hatfield, 1955], and the 1961 SL-1 accident in Idaho Falls, USA [McKeown, 2003], both of which resulted in severe damage and disruption of the reactor. These early reactivity initiated accidents led to design improvements, which were implemented in later generations of research reactors and, more importantly, in commercial power generating reactors. The design philosophy was to reduce potential causes for RIAs to a minimum, and if an accident still occurred, to quickly terminate the power surge[Glasstone & Sesonske, 1991]. Moreover, some scenarios for reactivity initiated accidents were identified by regulatory bodies as design basis accidents.

Notwithstanding the lessons learned from early research reactors, reactivity initiated accidents have still occurred in research reactors, military reactors and civil power generating reactors over the last fifty years. For example, a serious accident occurred on board the K-431 Russian Echo-II nuclear powered submarine at the Chazhma Bay naval facility near Vladivostok, Russia, in August 1985 [Takano et al, 2001]. The accident was caused by inadvertent rapid withdrawal of all control rods during reactor refuelling [Takano et al, 2001], leading to a hefty power pulse, steam explosion and subsequent fire. Ten people were killed immediately upon the explosion, but the radiological consequences of the accident were limited, since the PWR-type reactor core was loaded entirely with fresh fuel when the accident occurred [Takano et al, 2001].

The reactivity initiated accident that occurred in reactor 4 of the Chernobyl nuclear power plant, Ukraine, on April 26, 1986, is unprecedented with respect to radiological consequences and fatalities [IAEA, 1992]. The reactor, which was of light water graphite moderated pressure tube design (RBMK), was completely disrupted, and radioactively contaminated fallout spread over most of the northern hemisphere. The severe consequences of the Chernobyl accident were due to the fact that RBMKs lack not only a reactor containment, but also some of the inherent feedback mechanisms mentioned above for PWRs and BWRs [IAEA, 1992]. It should also be remarked that the accident occurred under a reactor test, where normal operating guidelines were ignored and safety systems were shut off.

The Chernobyl accident prompted new research into reactivity initiated accidents. Utilities and safety authorities in many countries undertook reviews of potential RIAs in their own power plants, and in

the early 1990s, experimental programs were also initiated in France, Japan and Russia to study the behaviour of highly irradiated nuclear fuel under reactivity initiated accidents. These test programs were primarily intended to check the adequacy of existing regulatory acceptance criteria for RIA, which at the time were based largely on test results for un-irradiated or moderately irradiated fuel. The extension of the experimental database to higher fuel burnup revealed that high burnup fuel exhibited different failure behaviour than fresh fuel, and that the susceptibility to fuel rod failure increased with increasing burnup. Hence, revisions of existing acceptance criteria were needed. These revisions, as well as the experimental programs, are still ongoing. Much of the experimental work is carried out in international programs, and the results are shared through expert meetings and seminars arranged by international organizations, such as the International Atomic Energy Agency (IAEA) and the Nuclear Energy Agency of the Organisation for Economic Co-operation and Development (OECD).

1.1 Consequences of reactivity initiated accidents

Reactivity initiated accidents lead to a fast rise in fuel power and temperature, which may cause failure of the nuclear fuel rods and release of radioactive material into the primary reactor coolant. This material comprises gaseous fission products as well as fuel pellet solid fragments. In severe cases, the fuel rods may be shattered, and large parts of the fuel pellet inventory dispersed into the coolant. The expulsion of hot fuel into water has potential to cause rapid steam generation and pressure pulses, which could damage nearby fuel assemblies, other core components, and possibly also the reactor pressure vessel. The current understanding of these damage mechanisms is based on RIA simulation tests, carried out on short-length fuel rods in dedicated pulse irradiation reactors. To date, more than a thousand pulse irradiation tests of this kind have been carried out on fresh (un-irradiated) fuel rods, and about 150 tests have been done on pre-irradiated samples.

The pulse irradiation tests have shown that fuel rods may fail by several damage mechanisms, depending on the characteristics of the thermal-mechanical loading and the state of the fuel: the thermal-mechanical loading depends on the accident scenario, while the state of the fuel depends mainly on fuel burnup and the reactor operating conditions when the accident occurs. A general observation from the tests is that the degree of fuel rod damage correlates with the peak value of fuel pellet specific enthalpy; the higher the enthalpy, the more extensive is the damage. The fuel specific enthalpy, i.e. the enthalpy per unit mass of the fuel pellet material, is therefore a fundamental parameter in discussions of reactivity initiated accidents. As long as the fuel is in solid state, its specific enthalpy, h_f, is simply calculated from the fuel temperature, T_f, through

Eq. 1-1: $$\boldsymbol{h_f(T_f) = \int_{T_0}^{T_f} c_f(T)\,dT}$$

where c_f is the specific heat capacity of the solid fuel and T_0 is a reference temperature at which h_f=0. In this report, we use T_0=273K. Terminology in engineering literature is a bit slack, and the word "specific" in specific fuel enthalpy is mostly left out for brevity.

Pulse irradiation tests generally show that cladding failure occurs at lower fuel enthalpies for irradiated than for fresh fuel rods, and that the susceptibility to failure increases with increasing fuel burnup. Moreover, failures of high burnup fuel rods usually occur at an early stage of the power surge, when the cladding temperature is low. The increased susceptibility to failure and the change from high temperature failures to a low-temperature failure mode are attributed to the combined effects of cladding tube embrittlement and aggravated pellet-cladding mechanical interaction in high-burnup fuel rods. It is also clear that the burnup dependent state of the rod, and in particular the degree of cladding waterside corrosion, is very important for survivability of pre-irradiated fuel rods.

Regulatory acceptance criteria for reactivity initiated accidents are commonly defined in terms of limits on the radially averaged fuel pellet specific enthalpy, or the increase of this property during the accident. The acceptance criteria vary with country and reactor type, but regulatory authorities usually postulate two kinds of enthalpy limits: (i) a definite limit for core damage, which must not be transgressed at any axial position in any fuel rod in the core, and (ii) a fuel rod failure threshold, that define whether a fuel rod should be considered as failed or not in calculations of radioactive release (source term). The core damage limit is to ensure integrity of the reactor coolant pressure boundary and maintenance of core coolability in the event of an accident, and it is generally formulated so that

2 Overview of RIA scenarios

There is a wide spectrum of scenarios for accidents and events that may result in inadvertent insertion of reactivity in nuclear power reactors. A general overview and classification of these scenarios in light water reactors are given in section 2.1. Two accident scenarios are of particular interest: the control rod ejection accident (CREA) in PWRs and the control rod drop accident (CRDA) in BWRs. These are design basis accidents, i.e. postulated events of low probability, which would have serious consequences if they were not inherently accounted for in the design of the reactor and related safety systems. Section 2.2 deals with the power pulses that are generated in these design basis accidents. We consider in particular the shape, amplitude and duration of the pulses, since these parameters are important to the fuel behaviour in an RIA; see section 6.2.

A very brief introduction to reactor kinetics, relevant to reactivity initiated accidents, is given in Appendix A. This introduction is strongly recommended for readers that are unfamiliar with the subject, since it provides a background to essential concepts like criticality, reactivity and reactivity feedback effects.

2.1 Overview of reactivity insertion events

Reactivity insertion events in power reactors can be divided principally into: (i) control system failures, (ii) control element ejections, (iii) events caused by coolant/moderator temperature and void effects, and (iv) events caused by dilution or removal of coolant/moderator poison. In the following subsections, we discuss events belonging to each of these classes for light water reactors. The presentation is based largely on a study of reactivity accidents by the International Atomic Energy Agency [IAEA, 1993].

2.1.1 Control system failures

All major types of power reactors use control elements (rods) for shutdown, and most reactors also use these rods for power control under normal operation. The control rods contain a neutron absorbing material, usually some of the elements B, Ag, Cd, In or Hf, which lowers the reactivity when the rods are inserted into the core. Inadvertent withdrawal of these rods, either due to control system faults or operator errors, is a possible cause to reactivity initiated accidents in all types of power reactors. However, reactor control systems generally place constraints on allowable control rod movements, thereby excluding operator errors as long as the control systems function well. Further protection is provided by operating limits, known as rod insertion limits (RILs), which put restriction on the reactivity worth[2] of each control element. Hence, should a control rod be inadvertently withdrawn, the RILs ensure that the reactivity addition will be manageable. Events involving inadvertent removal of control rods are generally not classified as accidents, but fall into the category of anticipated transients (Condition II events) [IAEA, 1993].

2.1.2 Control rod ejections

A control rod ejection can occur by mechanical failure of the control rod drive mechanism or its housing. As a consequence of the rod ejection, the reactivity of the core is rapidly increased due to decreasing neutron absorption. Since the reactivity addition rates and the resulting power transients are much larger for these events than for other reactivity accident scenarios, control rod ejections belong to the category of design basis accidents in light water reactors. This means that they are postulated, credible accidents with low probability that are used to establish the design basis for the reactor and to define safety limits for its operation. The postulated accident scenarios for control rod ejections in PWRs and BWRs are further described below.

[2] The change in reactivity that a control rod can produce by changing its axial position in the core.

2.1.2.1 Control rod ejection accidents in PWRs

The design basis reactivity accident in pressurized water reactors is the control rod ejection accident, usually referred to as CREA or REA. This accident is caused by mechanical failure of a control rod mechanism housing, such that the coolant pressure ejects a control rod assembly completely out of the core. The consequence of the control rod ejection is a rapid positive reactivity addition, which results in a core power excursion with large localized relative power increase [Diamond et al, 2002]. The rod ejection and its associated addition of reactivity to the core occur within about 0.1 s in the worst possible scenario; the actual time depends on reactor coolant pressure and the nature of the mechanical failure.

The nuclear design of the core affects the severity of the accident via the reactivity worth, location, and grouping of control rods. During normal operation of a PWR at full power, only one bank (group) of control rods is positioned in the core, and these rods are for safety reasons only partially inserted in the top of the core. This positioning is possible because reactivity changes under operation, e.g. caused by core depletion and xenon transients, are in a PWR compensated for by changes in the soluble boron concentration rather than by control rod movements. The amount of reactivity that is added by the ejection of a control rod during normal full power operation is thereby limited. At lower power, PWRs are allowed to operate with more banks and control rods further inserted. With respect to reactivity addition, the most severe CREA would therefore occur at hot zero power (HZP) conditions[3], i.e. with the coolant at normal reactor operating temperature and pressure, but with nearly zero reactor power [Diamond et al, 2002]. This accident scenario is further discussed in section 2.2.

2.1.2.2 Control rod drop accidents in BWRs

The design basis reactivity accident in boiling water reactors is the control rod drop accident, usually referred to as CRDA or RDA. The initiating event for this accident is the separation of a control rod blade from its drive mechanism. The separation is assumed to take place when the blade is fully inserted in the core, and the detached blade remains stuck in this position until it suddenly becomes loose and drops out of the core in a free fall. Hence, the control rod is removed from the core due to gravity, and in contrast to the CREA in PWRs, the accident can occur at any reactor operating condition, independent of coolant pressure, and the coolant pressure does not influence the rod ejection rate. More precisely, the control rod falls with a speed determined by the gravitational constant, corrected for buoyancy and water friction (the typical downward acceleration is 7.0–8.5 ms^{-2}). This makes the rod ejection slower in CRDAs than in CREAs. For this reason, and because of the coarser core lattice (lower ratio of fissile to non-fissile core material) for BWRs in comparison with PWRs, the power surge is generally somewhat slower in CRDAs than in CREAs; see section 2.2.1.

The power surge is terminated mainly by the negative fuel temperature feedback, see Appendix A, but if the coolant is saturated or close to saturation, additional negative feedback from coolant heating and vapour generation will help mitigate the power excursion. However, the reactivity feedback provided by changes in coolant temperature and vapour content is slower than the fuel temperature effect, since there is a time lag in fuel-to-coolant heat transfer. With respect to reactivity addition, the most severe CRDA is deemed to occur at cold zero power (CZP) conditions, i.e. at a state with the coolant close to room temperature and nearly zero reactor power [Dias et al, 1998; Gómez et al, 2005; Heck et al, 1995]. This accident scenario is further discussed in section 2.2.

2.1.3 Coolant/moderator effects

As indicated by Equation 1 in Appendix A, inadvertent changes in coolant/moderator temperature and/or void fraction may add reactivity to the core. Since the moderator temperature coefficient

[3] With respect to potential fuel damage, however, other operating conditions than HZP could be more challenging.

($\partial\rho/\partial T_m$) and void coefficient ($\partial\rho/\partial\alpha_m$) can have both positive and negative sign, scenarios for reactivity addition through moderator temperature and void effects vary significantly between reactors.

Pressurized water reactors are operated with a negative moderator temperature coefficient, but the coefficient may turn slightly positive in cases when the reactor is at zero power and the coolant is strongly borated and at low temperature. With the exception of these cases, reactivity can thus be inserted by a drop in coolant temperature. Possible scenarios for such an inadvertent event are the start-up of an inactive reactor coolant pump in an idle steam generator loop, or a sudden increase in heat removal by the secondary side [IAEA, 1993]. These events lead to relatively slow additions of reactivity, and they are classified as transients rather than accidents.

Boiling water reactors are operated with negative reactivity feedback from moderator temperature and void fraction, meaning that a reduction of these quantities results in reactivity addition to the core. Possible scenarios for reactivity events in BWRs include loss of feedwater heating, leading to coolant temperature reductions, and accidental operation of emergency core cooling systems or various over-pressurization transients, resulting in void collapse [IAEA, 1993]. These events are classified as transients rather than accidents, since they lead to relatively slow reactivity additions, which are unable to cause prompt criticality; see Appendix A.

Finally, it should be pointed out that both PWRs and BWRs use soluble neutron absorbers (poisons) in the coolant/moderator as a safety shutdown system, in complement to the control rods. Once this safety system is actuated, positive reactivity may be inadvertently added if the poisoned coolant/moderator is diluted with un-poisoned water. Scenarios for this kind of reactivity insertion events, which thus take place after reactor shutdown, often involve injection of un-poisoned water by the emergency core cooling system [IAEA, 1993]. . It should be remarked that PWRs use neutron absorbing boron in the primary coolant system as a means of reactivity control also under normal reactor operation. A malfunction of the chemical and volume control system (CVCS) that keeps the boron concentration in the reactor at its setpoint could therefore lead to inadvertent reactivity addition also under normal operation for PWRs.

2.2 Expected power pulse characteristics for various accident scenarios

Among the reactivity insertion scenarios reviewed in section 2.1, the control rod ejection accident in PWRs and the control rod drop accident in BWRs are of particular concern, since they may lead to fast and significant power excursions in fuel elements close to the failed control rod. The characteristics of the power pulse depend on the accident scenario - most importantly the reactivity worth of the ejected control rod, but also on the core and fuel design, reactor operating state, and the time at which the accident occurs under the fuel cycle [Riverola et al, 2004]. The reactivity worth of the ejected control rod depends on its position and insertion depth in the core, the core axial power shape and the fuel burnup distribution close to the ejected rod. A control rod ejected from a position dominated by high-burnup fuel gives a lower reactivity addition than if the rod is ejected from a position with fresh (un-irradiated) or low-burnup fuel.

Since the CREA and the CRDA are design basis accidents in PWRs and BWRs, respectively, these accident scenarios have over the years been closely analysed by use of computer codes and models. The rigour of the applied computational analyses and models varies, but they usually include neutron kinetics calculations coupled with calculations of fuel rod thermal-mechanics and coolant thermal-hydraulics, in order to capture the reactivity feedback effects from fuel and coolant heating. Moreover, a gradual shift from codes with lower dimensionality to three-dimensional models have taken place during the last decade, since the CREA and CRDA involve localized reactivity addition to the core.

Table 2-1 summarizes estimated values for the pulse width and maximum fuel pellet specific enthalpy under CREAs and CRDAs. The data are taken from realistic and moderately conservative analyses of postulated accident scenarios in reactor cores with UO_2 fuel, which have been carried out with state-of-the-art computer codes and reported in open literature. It should be noted that the behaviour of $(U,Pu)O_2$ mixed-oxide fuel and thorium bearing fuel during reactivity initiated accidents is different from that of UO_2 fuel; see Appendix A. The fuel pellet enthalpies reported in Table 2-1 pertain to the

3 Overview of damage phenomena

3.1 Types of damage to fuel and cladding

As will be shown in section 4.1, it is known from RIA simulation experiments in power pulse reactors that the fuel rod behaviour under an RIA is affected primarily by the [Organisation for Economic Co-operation and Development (OECD), 2010]

- Characteristics of the power pulse, in particular the amplitude and pulse width.
- Core coolant conditions, i.e. the coolant pressure, temperature and flow rate.
- Burnup-dependent state of the fuel rod. Among the most important properties are the pre-accident width of the pellet-cladding gap, the degree of hydrogen pickup through the cladding waterside corrosion), the internal gas overpressure in the fuel rod, and the distribution of gaseous fission products in the fuel pellets.
- Fuel rod design. Parameters of particular importance are the internal fill gas pressure, cladding tube wall thickness, fuel pellet composition ($UO_2/PuO_2/Gd_2O_3$, enrichment) and the fuel pellet geometrical design (solid/annular).

These factors are important to the fuel rod behaviour during an RIA, and they also control what kind of damage may be inflicted to the fuel rod under the accident (Figure 3-1 and Figure 3-2). The rapid increase in power under the RIA leads to nearly adiabatic heating of the fuel pellets, which immediately deform by solid thermal expansion. If the fuel has been operated for some time and gaseous fission products are retained in the fuel, the expansion of the accumulated gas will add to the solid pellet deformation.

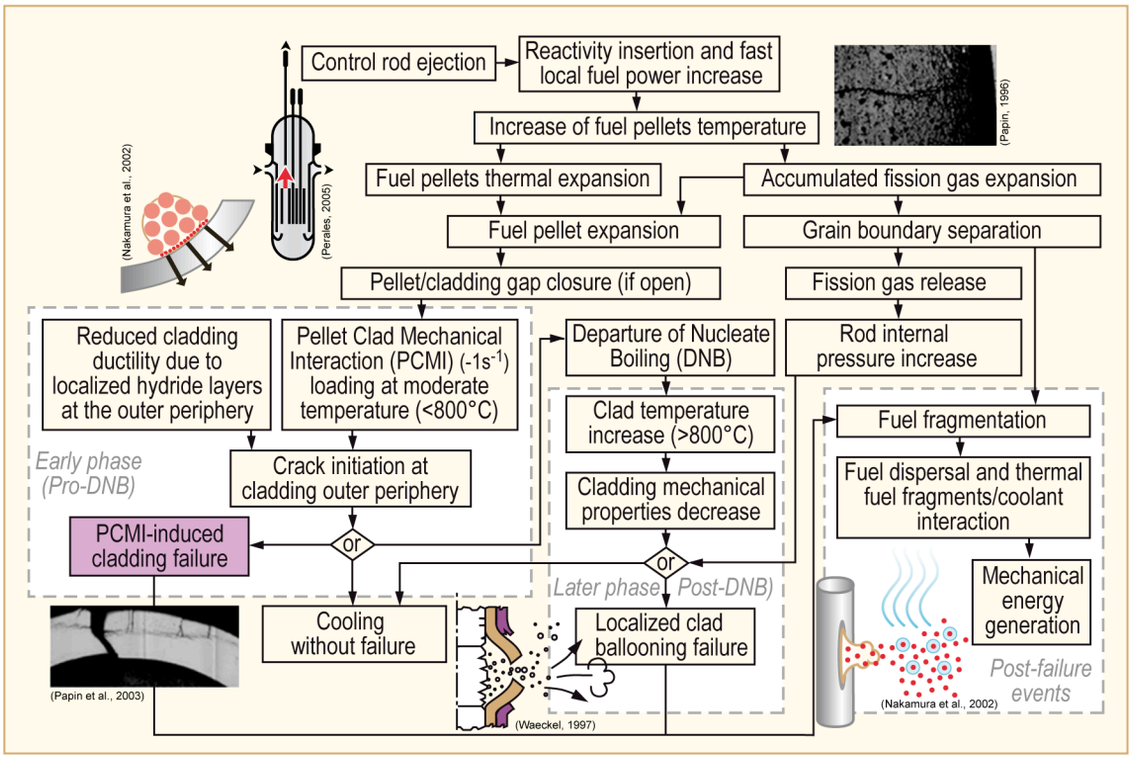

Figure 3-1: Effects of a RIA on fuel [Le Saux et al, 2007].

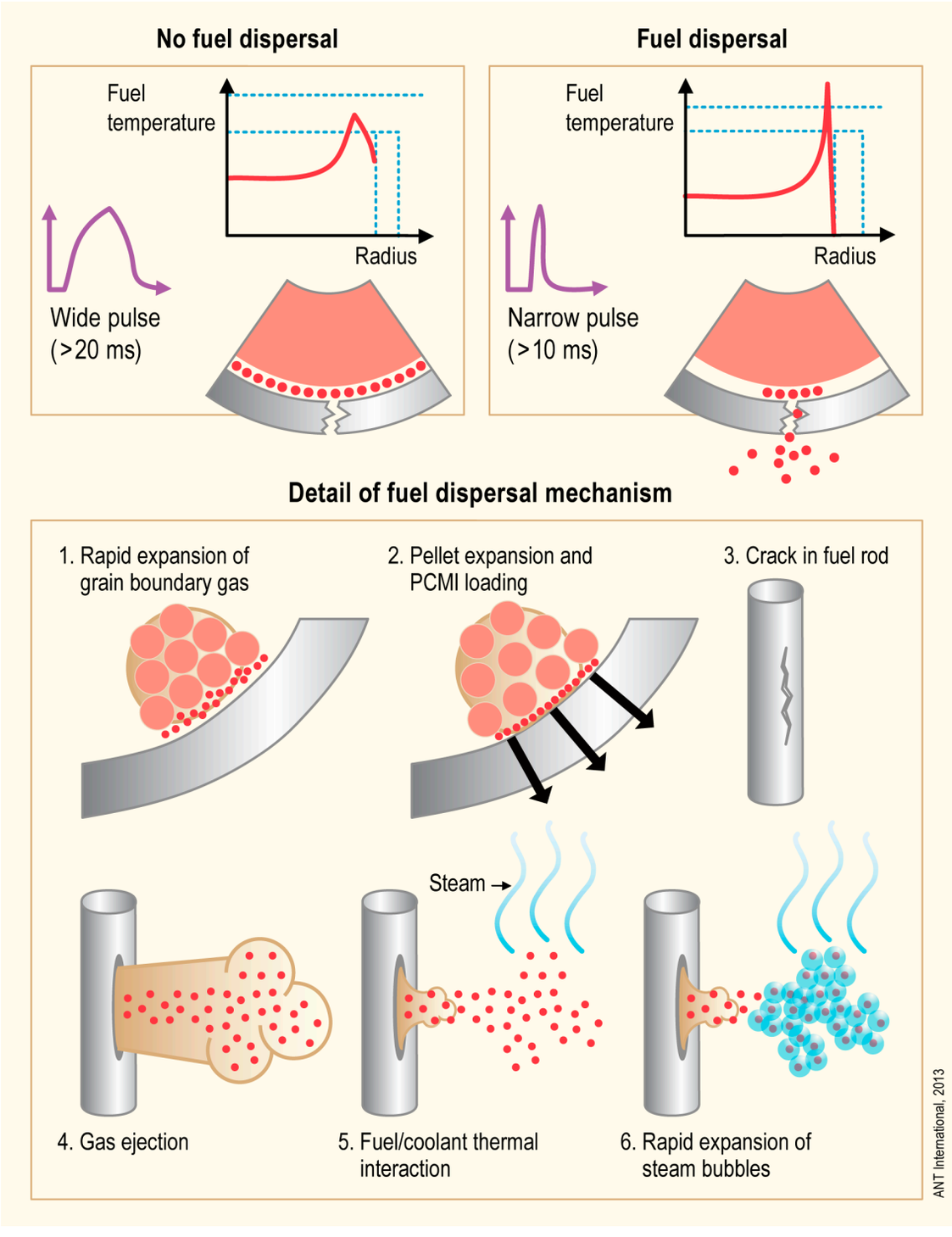

Figure 3-2: Impact of pulse width on high burnup fuel.

In case the pellet-cladding gap is narrow or closed, which is normally the case for high-burnup fuel, pellet-cladding mechanical interaction (PCMI) will lead to rapid and biaxial mechanical loading of the cladding tube. At this early stage of the accident, the cladding material is still at a fairly low temperature, and the thrust imposed by the expanding fuel pellets may therefore cause a partially brittle mode of cladding failure [Chung & Kassner, 1998]. This low-temperature failure mode is commonly observed in pulse irradiation tests on high-burnup fuel rods.

At a later stage of the transient, heat transferred from the pellets may bring the cladding to such a high temperature that a boiling crisis occurs. This is sometimes referred to as departure from nucleate

boiling (DNB) and involves formation of a continuous vapour film at the cladding-to-coolant interface, which effectively insulates the cladding from the coolant [Ruyer, 2016]. This condition is called film boiling. If it occurs, RIA simulation tests in pulse reactors suggest that the cladding material can remain at high temperature for up to about 15 s, until re-wetting takes place. This fairly long period at elevated temperature may lead to cladding ballooning and creep rupture, in cases where significant pressure differences exist across the cladding wall. As indicated in Figure 3-1, transient release of accumulated fission gas increases the internal pressure loading.

Another mode of high-temperature failure may occur by thermal shock during re-wetting of the overheated cladding tube, since thermal stresses under the abrupt quenching may cause brittle fracture and disruption of the cladding material. This failure mode is imminent if the cladding tube is embrittled by high temperature oxidation during the film-boiling phase.

Finally, if the energy deposited to the fuel is very high, the cladding and possibly also the fuel pellets may melt. Melting has been observed in pulse irradiation experiments on test rods charged with highly enriched fuel (10–20 wt% ^{235}U). The melting generally leads to cladding failure and violent thermal interaction between molten material and the coolant, causing pressure pulses in the coolant. For typical LWR fuel, the enrichment is significantly lower (< 5 wt%), and the energy deposition required for melting cannot be achieved in the experimental facilities at hand. This pertains in particular to high-burnup fuel. However, thermal interaction between non-molten fuel fragments and the coolant may occur, as indicated in the rightmost column of Figure 3-1. This process is important to high-burnup fuel, in which decohesion of the gas-filled grain boundaries turns the outer part (rim) of the fuel pellet into fine fragments during the RIA. Fuel-coolant interaction and its consequences are further discussed in section 3.3 below.

Based on the results of integral RIA simulation tests, fuel rod failures are usually divided into:

- Low temperature failures, induced by pellet-cladding mechanical interaction (PCMI), which occur under the early heat-up phase of the accident.
- High temperature failures, which occur at a later stage of the accident, as a result of film-boiling, degraded clad-to-coolant heat transfer and a prolonged period with overheated cladding.

Low temperature PCMI-induced cladding failures under RIA may occur in high-burnup fuel rods, but not in fresh or low-burnup rods. This failure mode is more likely for accidents that initiate from conditions with low reactor power and/or low coolant temperature than for accidents that occur at full reactor power. The PCMI-induced low temperature failures generally occur at significantly lower fuel enthalpies than high temperature failures.

High temperature fuel rod failures under RIA may occur by three different modes: (i) cladding ballooning and burst, (ii) fuel rod disruption upon quenching, and (iii) cladding melting. The first of these failure modes is limiting when there is a substantial gas overpressure in the fuel rod. Fuel rod disruption under quenching is due to cladding embrittlement by high temperature oxidation under the film-boiling phase. This failure mode was frequently observed in early pulse reactor tests on fresh and low-burnup fuel rods, when the fuel enthalpy reached about 240 cal$(gUO_2)^{-1}$, i.e. about 1000 J$(gUO_2)^{-1}$. Early acceptance criteria for RIA in light water reactors were based largely on this threshold enthalpy.

The different mechanisms for cladding failure are discussed more in section 5.

3.2 Phenomena with influence on core coolability

As mentioned in section 1, regulatory acceptance criteria for RIA in light water reactors are intended to ensure long-term core coolability and to preclude damage to the reactor pressure vessel. Scenarios for loss of long-term core coolability after an RIA involve loss of coolable fuel geometry, for instance by ballooning or fragmentation of the fuel rods. Coolable fuel geometry may also be lost even if a rod-like geometry is preserved, in case large amounts of fuel pellet fragments are dispersed into the coolant

4 Integral RIA simulation tests and separate effect tests

The fuel behaviour during reactivity initiated accidents has over the years been studied by integral RIA simulation tests, performed on instrumented short-length rodlets in dedicated power pulse reactors, and by separate effect tests, in-reactor or ex-reactor, on fuel or cladding samples. The pulse reactor tests are done at conditions that approximate those expected in power reactors under RIA, and they provide valuable information on the integral fuel rod behaviour under the accident. However, there is currently a lack of experimental facilities, in which integral RIA simulation tests can be carried out. Moreover, the integral tests are costly, and it is also difficult to investigate isolated phenomena and/or the role of particular parameters by in-reactor experiments. Ex-reactor separate effect tests, performed under well-controlled conditions, are therefore needed to investigate e.g. cladding mechanical properties, cladding-to-coolant heat transfer and fuel fission gas release under conditions expected in RIAs. The following subsections provide an overview of RIA integral and separate effect tests, performed up to 2016. A more detailed presentation of integral RIA simulation tests on pre-irradiated fuel is given in Appendix B -.

4.1 Integral RIA simulation tests

As mentioned in section 1, the main safety concerns in reactivity initiated accidents are loss of long-term core coolability and possible damage to the reactor pressure boundary and to the core through pressure wave generation. Fuel failure, i.e. loss of cladding tube integrity, is in itself generally not considered a safety concern, since fuel failures do not necessarily imply loss of coolable geometry or generation of harmful pressure waves. Nonetheless, integral RIA simulation tests in dedicated power pulse reactors have historically been focused on fuel rod failure. The reason is that fuel rod failure is a prerequisite for loss of coolable core geometry and pressure wave generation, and that many regulators require that the number of failed fuel rods in the core should be calculated in evaluations of radiological consequences to design basis RIAs.

4.1.1 Overview of pulse reactor tests

4.1.1.1 Tests on fresh fuel rods

A large number of RIA simulation tests have been performed on fresh (un-irradiated) LWR fuel rods, using pulse reactors in the USA, Japan, Russia and Kazakhstan. These tests, which were carried out predominantly from the sixties to the eighties, can largely be divided into two groups:

- Tests done to establish thresholds, in terms of peak fuel enthalpy, for cladding failure, fuel dispersal, melting, etc. Since these tests are generally aimed at establishing acceptance criteria for RIAs in power reactors, the tests are done on fuel rods of prevalent commercial design and under conditions that, as closely as possible, resemble those expected for power reactor RIAs.

- Parametric studies, intended to shed light on the fuel behaviour and mechanisms of fuel failure under RIAs, and to generate data needed for verification and calibration of computer codes. The effects of selected parameters are studied by performing series of tests, in which a single parameter of interest is varied at a time. The impact of fuel rod design parameters as well as power pulse characteristics and reactor coolant conditions has been studied in this manner.

Reviews of these early RIA simulation tests on fresh fuel rods are available in literature, e.g. [Asmolov & Yegorova, 1996; Ishikawa & Shiozawa, 1980; Ishikawa et al, 1989; Liimatainen & Testa, 1966; MacDonald et al, 1980]. Table 4-1 summarizes the characteristics of seven pulse reactors, which have been used for RIA simulation tests of fresh LWR fuel rods. The SPERT and PBF reactors have been decommissioned, TREAT is planned to be taken into operation in 2018 after being shutdown from 1994, and the other reactors listed in Table 4-1 are still in operation [IAEA, https://www.iaea.org/OurWork/ST/NE/NEFW/Technical-Areas/RRS/databases.htmls]. The type of fuel tested in each reactor is also indicated in Table 4-1. A few fresh fuel rods with MOX [Abe et al, 1992], rock-like oxide (ROX) inert matrix fuel (IMF) [Nakamura et al, 2003] and burnable absorber (BA) [Shiozawa et al, 1988] fuels have been tested, but apart from these exceptions, the tests have been done

on rods with UO_2 fuel. The UO_2 test rods were often, but not always, loaded with fuel pellets enriched to higher fractions of ^{235}U than typically used in commercial fuel rod designs. This is necessary in some of the pulse reactor facilities in order to increase the energy deposition to levels where fuel rod fragmentation and melting occur; see section 3.2.2. The enrichment affects the radial distribution of power and temperature in the fuel pellet, and parametric studies in the NSRR have shown that increased enrichment lowers the enthalpy threshold for failure of fresh fuel rods [Ishikawa & Shiozawa, 1980].

Table 4-1: Overview of pulse reactor facilities used for RIA simulation tests on fresh LWR fuel rods. All pulse reactors used light water as coolant.

	TREAT US	**SPERT** US	**PBF** US	**IGR** KZ	**BIGR** RU	**HYDRA*** RU	**NSRR** JP
Test conditions							
Coolant temperature [K]	293	293	538	293	293	293	293–578
Coolant pressure [MPa]	0.1	0.1	6.45	0.1–16	0.1	0.1	0.1–16
Coolant flow [ms^{-1}]	0	0	0.5	0	0	0	0–1.8
Pulse width [ms]	350–1000	13–31	11–16	100–1000	2–3	4–8	4–7
Test rods							
Rod type	BWR	BWR	PWR	VVER	VVER	VVER	BWR PWR
Active length [mm]	140–240	≈ 130	≈ 1000	≈ 150	≈ 150	≈ 150	≈ 130
* The full name for the Russian HYDRA reactor is IIN-3M GIDRA.							
ANT International, 2016							

4.1.1.2 Tests on pre-irradiated fuel rods

A total of about 150 RIA simulation tests have under the past four decades been carried out on pre-irradiated LWR fuel rods. Most of these tests were done on UO_2 fuel rods, but 14 of the tests pertain to $(U,Pu)O_2$ mixed oxide fuel. Six different pulse reactors have been used for the testing, and in two of them, RIA simulation tests are still being conducted, as follows:

- SPERT-CDC (Special Power Excursion Reactor – Capsule Driver Core, Idaho Falls, ID, USA). Experiments performed in 1969–1970.
    - Special Power Excursion Reactor – Capsule Driver Core. Experiments performed in the United States 1969–1970. The general objective of the tests was to obtain safety-related data on fuel rod behaviour during an RIA [MacDonald et al, 1980]. The experimental program included un-irradiated test rods, as well as test rods pre-irradiated in the Engineering Test Reactor (ETR) to rod average burnups in the range of 1 to 33 MWd/kgU. The SPERT experiments with 132 mm Zry-2 test rods simulated the conditions of a BWR during cold startup (atmospheric pressure at 298K, with no forced coolant flow and zero initial power). The pulse widths were in the range of 13 to 31 ms.

- PBF (Power Burst Facility, Idaho Falls, ID, USA). Experiments performed in 1978–1980.
    - The PBF experiments simulated the hot startup conditions in a BWR, i.e. water temperature 559K and pressure 7.0 MPa, using individually shrouded fuel rods at relatively low burnups, [MacDonald et al, 1980].
- IGR (Pulse Graphite Reactor, Kurchatov, Kazakhstan). Experiments performed in 1990–1992.
    - The Russian IGR in Kurchatov Semipalatinsk, Kazakhstan, is a uranium-graphite reactor with a central experimental hole for uninstrumented experiments with a pulse width of 630–850 msec. From 1990 to 1992, tests were done on pre-irradiated VVER rods [Yegorova, 1999]. Rodlets were re-fabricated from full-length VVER rods with burnups in the range of 47 to 49 MWd/(kgU). The cladding oxide layer was only about 5 μm (and negligible fuel clad hydrogen content) thick for the pre-irradiated test rods, in spite of their fairly high burnup.
- BIGR (Fast Pulse Graphite Reactor, Sarov, Russia). Experiments performed in 1997–2000.
    - The BIGR is another uranium-graphite pulse reactor that has been used for RIA simulation tests of VVER fuel rods. Single rods are tested in a capsule with water under ambient conditions (20°C and 0.1 MPa). The BIGR reactor has a natural pulse width of 2–5 ms. From 1997 to 2000, tests were carried out on pre-irradiated VVER fuel ranging in burnup between 47 and 60 MWd/(kgU) [Yegorova et al, 2006].
- NSRR (Nuclear Safety Research Reactor, Tokai, Japan). Ongoing experiments, carried out since 1975.
    - The Japanese NSRR is located in Tokai. The NSRR facility has a TRIGA-ACPR[9] pool reactor, which generates significantly narrower power pulses than expected under RIA in LWRs. The reactor and reactivity control system yield pulses with full width at half maximum in the range of 4.4 to 7 ms. Irradiated fuels have been tested since 1975 in instrumented capsules containing stagnant water at atmospheric conditions at room temperature (RT) conditions. However, a new test capsule, allowing high coolant temperature and pressure, was taken into operation in 2005 [Fuketa et al, 2006]. The high-temperature (HT) capsule operates with an electric heater surrounding the specimen and 6-7 MPa pressure on the coolant. The RT capsule is compared to the HT capsule in Figure 4-1.

[9] Training, Research, Isotopes General Atomics – Annular Core Pulse Reactor (TRIGA-ACPR). TRIGA is a class of small research reactors, designed and manufactured by General Atomics, USA.

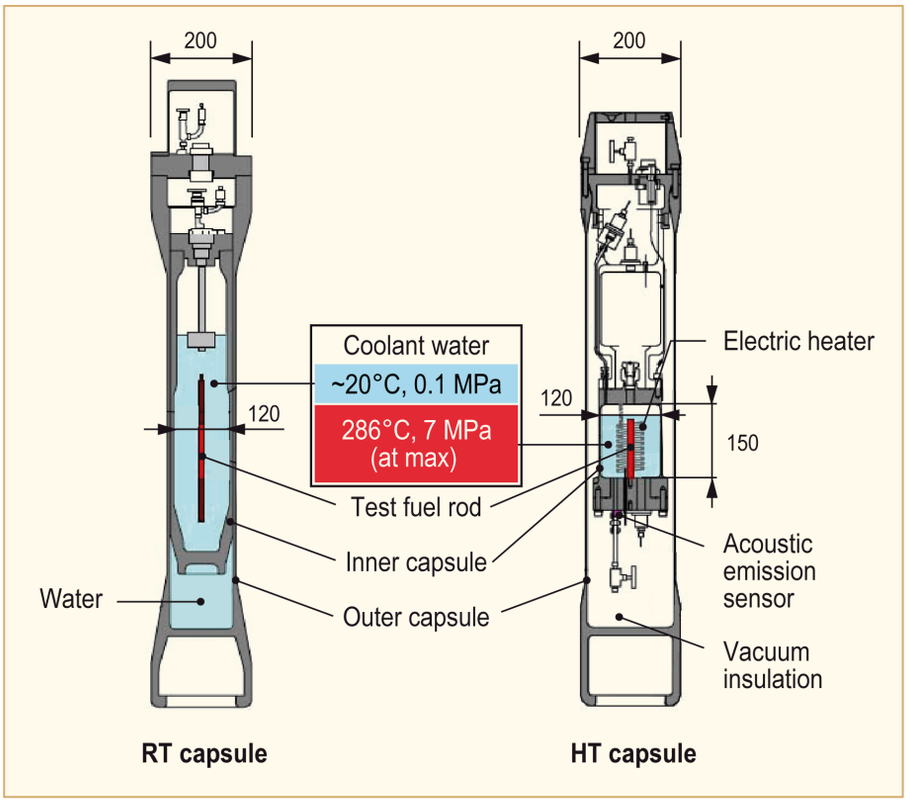

Figure 4-1: Schematics of NSRR RT and HT test capsules [Sugiyama et al, 2009].

The pre-irradiated test rods used in the NSRR tests can be separated into four main groups:

- PWR test rods,
- BWR test rods,
- Advanced Test Reactor (ATR) MOX test rods, and
- Japanese Material Test Reactor (JMTR) rods.

The first two groups of rods were sampled from full-length commercial fuel rods, which were irradiated in commercial power plants and then re-fabricated into short-length test rodlets. The third group of rods were re-fabricated from fuel rods operated in the ATR, Japan. The fourth group of test rods, which were pre-irradiated in the JMTR, were manufactured as short-length test rodlets, and directly inserted into the test capsule after pre-irradiation in the JMTR.

A total of 8 tests have been conducted with the HT capsule and compared to companion specimens in the RT capsule on fuel segments with the 6 currently used cladding alloys: Zircaloy 4, Zircaloy 2 (LK3[10] with liner), Zirconium Low Oxidation (ZIRLO), M5, Mitsubishi Developed Alloy (MDA) and Modified Mitsubishi Developed Alloy (M-MDA) . The burnup of these rods ranged from 59 to 81 GWD/MT. See Appendix B -.

- CABRI (Cadarache, France), Experiments performed in 1993–2002 with sodium coolant loop. Tests with water coolant loop planned to start in the near future.

[10] Låg Korrosion (Low Corrosion in Swedish)

5 Cladding failure mechanisms

There are four different fuel cladding failure mechanisms described in the following according to Clifford [Clifford, 2015] – these are the same failure modes as described in Section 3.1. However, to facilitate the understanding of the new proposed NRC regulation, Section 8.2 , the grouping of the failure mechanisms are different in this section:

1. Brittle Failures:
    a) Oxygen-induced embrittlement and fragmentation at high-temperature post-Departure from Nucleate Boiling (DNB) occurring at high temperatures
    b) Hydrogen-enhanced Pellet Cladding Mechanical Interaction (PCMI) cladding failure occurring at low temperatures
2. Ductile Failure: High-temperature fuel rod cladding creep ballooning and burst occurring at high temperatures
3. Fuel Melt: Molten fuel-induced swelling PCMI cladding failure occurring at high temperatures.

5.1 Brittle failure

5.1.1 Post-DNB failure-failure mechanism 1a

Post-DNB brittle fracture of the clad material occurring during the re-wetting phase of the overheated heavily oxidised (and thereby embrittled) clad due to the abrupt quenching resulting in large thermal clad stresses. At temperatures above 700°C zirconium alloy cladding is rapidly oxidized from both the UO_2-metal reaction on the inside surface and the water-metal reaction on the outside surface. Oxygen absorbed during the oxidation process embrittles the metal and thermal stresses that arise under quenching (re-wetting) may be sufficient to fracture the fuel cladding. Cladding fracture upon quenching from HT is largely controlled by:

- The brittleness of the oxidized material, where the degree of embrittlement depends principally on the oxygen concentration in the transformed β-phase zirconium.
- The magnitude of thermal stress in the cladding. The thermal stress is caused by temperature gradients in the material, and the magnitude of these gradients depends on the quench temperature.

This failure mode was frequently observed in early pulse reactor tests on un-irradiated fuel rods, when the fuel enthalpy reached about 240 cal$(gUO_2)_{-1}$ [Ishikawa & Shiozawa, 1980] and [MacDonald et al, 1980]. Early acceptance criteria for RIA in LWRs were based largely on this threshold enthalpy.

5.1.2 PCMI: Hydrogen-enhanced PCMI cladding failure-failure mechanism 1b

As the burnup increases the failure mode changes from post-DNB (and fuel melting) to PCMI failures during a RIA event for a fuel rod not subjected to DNB (Figure 5-1).

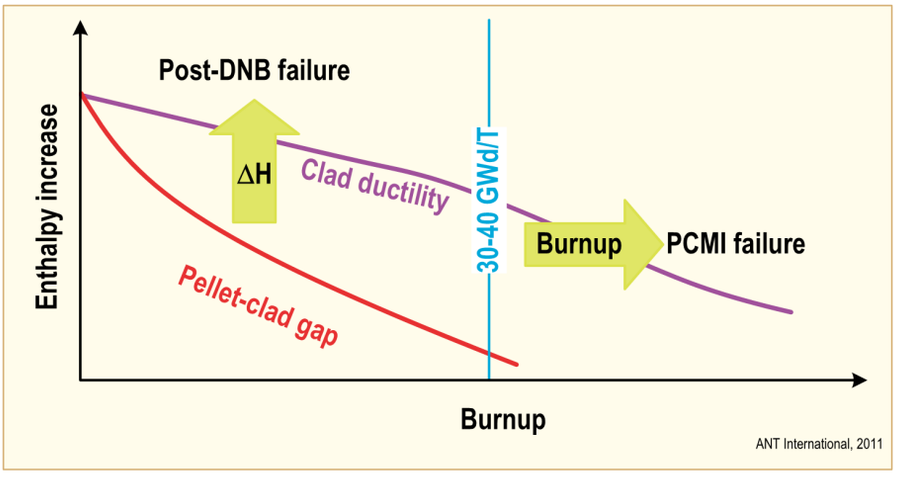

Figure 5-1: Clad failure mechanisms, modified figure according to [Montgomery et al, 2003].

The survival of a high burnup fuel rod under PCMI conditions in a RIA depends on:

- The imposed stress and stress state in the cladding. The stress level depends on the enthalpy increase and pellet-clad gap size prior to the RIA pulse (which decreases with burnup).
- The cladding ductility, which decreases with
  - The clad temperature which in turn is dependent on the pulse width, enthalpy increase of the transient and, heat transfer coefficient between coolant/clad oxide and coolant temperature.
  - The clad hydrogen content, the hydride orientation and distribution.

The PCMI sequence of events in a RIA transient can be summarised as follows:

- The fuel pellet expands rapidly due to thermal expansion during a RIA transient.
- Pellet-cladding gap affects PCMI on RIA:
  - At low burnups the gap is quite large and a quite high enthalpy increase is needed for gap closure.
  - With increasing burnup the gap between pellet and cladding decreases during base irradiation due to cladding creep down and fuel swelling, which decrease the enthalpy for gap closure.
  - At high burnup, the gap is closed and consequently, the PCMI will start very early in the transient, as the only space available is the residual gap created by the contraction of the pellet when power was reduced from operating level to zero (for hot-zero-power conditions).
- Enthalpy increase after gap closes impose stresses in the cladding, which may eventually fail due to PCMI. The PCMI stresses are generated primary by fuel pellet thermal expansion.

5.2 Ductile failure: Rod ballooning and burst-failure mechanism 2

At a later stage of the transient, heat transferred from the pellets may bring the clad outer surface to such a high temperature that a boiling crisis occurs, whereby a continuous vapour film with very low thermal conductivity forms at the cladding surface. If so, the clad material could remain at a

temperature above 1000-1200 K for up to 10 s, until rewetting takes place [Fuketa et al, 2007]. The elevated temperature may lead to *clad outward ballooning and creep burst*, in cases where the rod internal gas pressure exceeds the coolant pressure, which may be the case for some high burnup rods [Ishijima & Nakamura 1996], see Figure 5-2 and Figure 5-3.

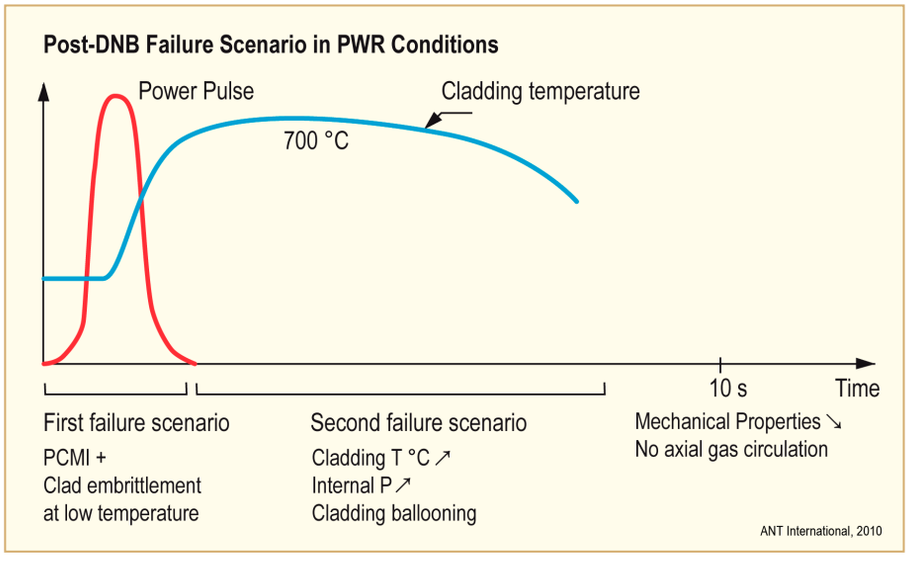

Figure 5-2: Post-dnb ductile failure scenario in PWRs for high burnup rods [Waeckel, 1997].

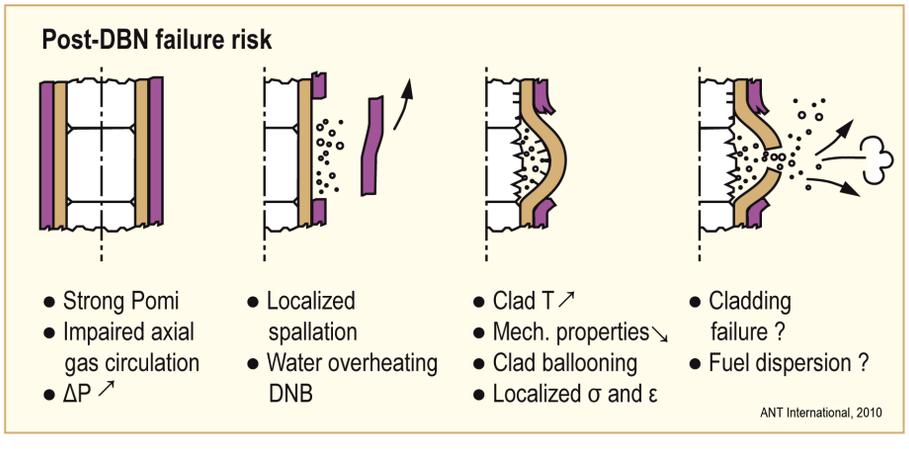

Figure 5-3: Post-dnb ductile failure scenario in PWRs for high burnup rods [Waeckel, 1997].

Burst-type cladding failures with un-irradiated, pre-pressurized fuel rods were studied in a series of NSRR experiments [Saito et al, 1982]. A failure threshold can be defined in terms of the peak fuel enthalpy and rod internal – external pressure difference, as shown in Figure 5-4. The dashed-line in the figure is a failure threshold derived from the NSRR experiments with a single test rod. When the pressure difference was below 0.6 MPa, cladding fractured with partial melting at a peak fuel enthalpy of 212 cal/g or higher. Above the difference of 0.6 MPa, the failure mode changes to creep burst and the threshold decreases with increasing pressure difference [Fuketa & Sugiyama, 2009].

At peak fuel enthalpy levels below 88 cal/g, DNB did not occur (and consequently no failure occurred). It turns out that these failures are strongly affected by rod cooling conditions and that the single-rod experiments give a less conservative threshold [Fuketa & Sugiyama, 2009]. In another test series with rod bundle geometry, a 15% reduction of the failure threshold due to the decreased coolability was observed. With the 15% reduction and a 10 cal/g margin, the acceptable fuel design limit was determined as a solid-line of Figure 5-4.

6 Parameters affecting RIA fuel performance

From RIA simulation experiments in power pulse reactors, the fuel rod behaviour under a RIA is primarily affected by the:

- Core coolant conditions, i.e. the coolant pressure, temperature and flow rate.
- Characteristics of the power pulse, in particular the amplitude and pulse width.
- Burnup-dependent state of the fuel rod. Among the most important properties are the pre-accident width of the pellet-clad gap, the degree of cladding embrittlement (through hydrogen pickup), the internal gas overpressure in the fuel rod, and the distribution of gaseous fission products in the fuel pellets.

6.1 CZP and HZP

With respect to reactivity addition in a PWR, the most severe CREA would occur at HZP conditions, i.e. at normal coolant temperature and pressure, but with nearly zero reactor power [Agee et al, 1995] and [Nakajima et al, 2002]. This is shown in Figure 6-1 where it appears that the rod worth[17] decreases with increased power level and with a decrease in control rod insertion within the core.

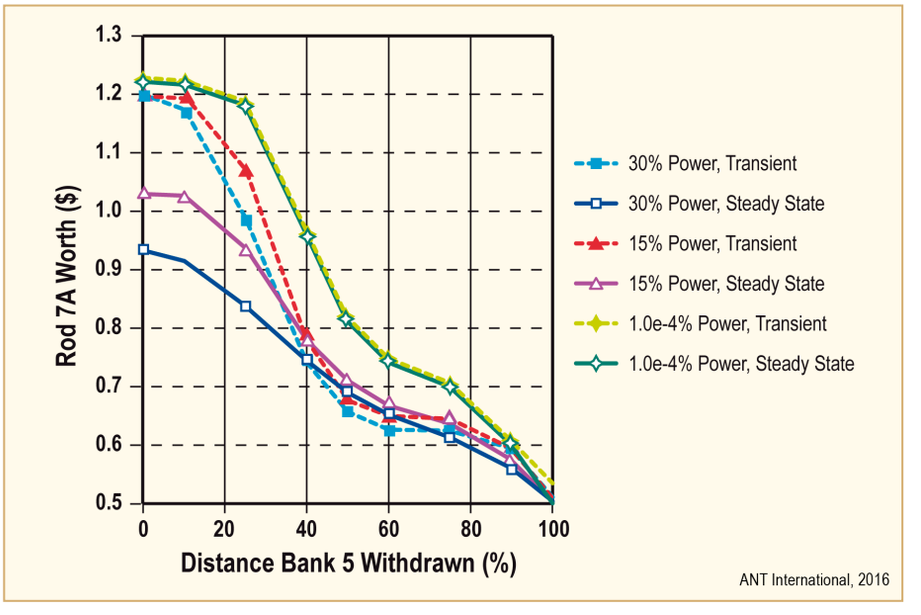

Figure 6-1: Three Mile Island (TMI-1) PWR End Of Cycle (EOC) control rod 7a worth variation with power level, bank 5 position, and calculation procedure [Diamond et al, 2001].

With respect to reactivity addition in a BWR, the most severe CRDA would occur at CZP conditions, i.e. at a state with the coolant close to RT and atmospheric pressure, and the reactor at nearly zero power [Agee et al, 1995] and [Nakajima et al, 2002]. The degree of reactivity addition during CRDA is strongly affected by the coolant subcooling, since vapour generation effectively limits the power transient.

[17] The control rod worth is roughly proportional to the square of the neutron flux at a given location. The rod worth is a measure for the step decrease (or prompt drop) in the reactivity when a rod is suddenly dropped a known distance into the core (PWR) or inserted into the core (BWR).

6.1.1 Effect on power pulse characteristics

Table 6-1 provides the estimated values for the pulse width and maximum fuel pellet specific enthalpy under CREAs and CRDAs. The data are taken from realistic and moderately conservative analyses of postulated accident scenarios, which have been carried out with state-of-the-art computer codes and reported in open literature.

Table 6-1: Estimated pulse widths and core-wide maxima of fuel pellet radial average enthalpy and enthalpy increase for various scenarios of CREA and CRDA. The data are compiled from realistic and moderately conservative computer analyses of cores with UO_2 fuel.

Reactor, accident scenario	**Pulse width** [ms]	**Max fuel enthalpy** [$J(gUO_2)^{-1}$]	**Max ent. increase** [$J(gUO_2)^{-1}$]	**Rod worth** [10^{-5}]	**Literature sources** [references]
PWR:					
CREA HZP	25–65	110–320	40–250	600–940	[9, 10, 14–18]
CREA HFP	400–4500	230–350	1–130	40–200	[10, 14, 17, 19–21]
BWR:					
CRDA CZP	45–75	140–460	130–450	700–1300	[10, 11, 14, 22]
CRDA HZP	45–140	160–00	90–320	600–1300	[10, 22, 23]
HZP: Hot zero power, **HFP**: Hot full power, **CZP**: Cold zero power					
ANT International, 2016					

Table 6-1 shows that increased coolant temperatures at CREAs results in both wider pulses and lower maximum fuel enthalpy increases. Thus, a CREA at HZP or a CRDA at CZP results in less margins to fuel failures and fuel dispersal than a CREA at HFP or a CRDA at HZP.

6.1.2 Effect on propensity for PCMI failures

The effect of increasing the coolant temperature on the tendency for PCMI failures in a fuel rod during a RIA event can be evaluated by comparing two sibling rods tested both at room temperature (RT) and high temperature (HT).

The first example is the two ZIRLO sibling rods, from Vandellos (VA-1) tested at RT and VA-3 tested at HT (Table 6-2).

Table 6-2: Fuel descriptions, test conditions and main observations in NSRR high/RT tests [Sugiyama et al, 2009].

ID for test and test fuel rod	VA-1	VA-3	VA-2	VA-4	RH-1	RH-2	LS-1	LS-2	BZ-2	BZ-3
Descriptions of mother fuel rod										
Reactor, country	Vandellos, Spain				Ringhals, Sweden		Leibstadt, Switzerland		Beznau, Switzerland	
Fuel type			17×17 PWR-UO_2				10×10 BWR-UO_2		14×14 PWR-MOX (MIMAS[2])	
Clad OD[1]/ID, mm			9.5/8.36				9.62/8.36		10.72/9.48	
Clad material	ZIRLO™		MDA		M5™		Zircaloy-2 (LK3) with Zr liner		Zircaloy-4	
Pellet burnup, GWd/t	71		77		67		69		59	
Description of test fuel rod										
Clad oxide thickness, µm	73	82	70	80	6	6	25	25	20	20
Clad hydrogen content, ppm	660	670	760	760	70	70	300	290	160	160
Pellet stack length, mm	112	61	111	61	117	50	107	52	110	51
Rod internal gas	helium of 0.1 MPa at ~20°C									
Test conditions										
Power pulse width, ms	4.4					4.5	4.4			
Initial coolant conditions	18°C 0.1 MPa	285°C 6.8 MPa	28°C 0.1 MPa	249°C 4.0 MPa	16°C 0.1 MPa	278°C 6.4 MPa	17°C 0.1 MPa	283°C 6.6 MPa	18°C 0.1 MPa	281°C 6.6 MPa
Initial fuel enthalpy, (20 °C-based), H_0, J/g (cal/g)	-	71(17)	-	61(14)	-	69(16)	-	70(17)	-	70(17)
Max. increase of fuel enthalpy, ΔH_{max}, J/g (cal/g)	556(133)	454(108)	546(130)	457(109)	462(110)	378(90)	469(112)	371(89)	644(154)	528(126)
Main results										
Enthalpy increase at failure, ΔH_{fail}, J/g (cal/g)	268(64)	344(82)	231(55)	no failure	no failure	no failure	222(53)	no failure	545(130)	no failure
Key observations	• PCMI failure • all pellets fragmented • mechanical energy detected	• PCMI failure • some pellets fragmented	• PCMI failure • all pellets fragmented • mechanical energy detected	• PCMI and gas-induced clad strain of 2.2%	• PCMI-induced clad strain of 0.96% • FGR 21.4%	• PCMI-induced clad strain of 1.06% • FGR 26.0% • DNB detected	• PCMI failure • all pellets fragmented • mechanical energy detected	• PCMI-induced clad strain of 0.93%	• PCMI failure • all pellets fragmented • mechanical energy detected	• PCMI and gas-induced clad strain of 4.4% • FGR 39.4% • DNB detected

1. Outer Diameter
2. Micronized master blend route

• ANT International, 2016

Both rods failed at similar peak enthalpies, but VA-3 failed at a higher fuel enthalpy increase of 82 cal/g (344 J/g) versus 64 cal/g (268 J/g) of VA-1. Both failed before the cladding temperature increased from their starting levels of about 20°C (VA-1) and 285°C (VA-3). Metallography indicated numerous cracks propagating from the oxide into the brittle hydride zone on the cladding OD and brittle fracture zones at the OD with ductile fracture at mid clad wall (Figure 6-2). The crack tips in the HT test appear rounded compared to the sharp tips of the RT test. The higher initial cladding temperature and the resulting increased fracture toughness is thought to have delayed crack propagation and resulted in a higher fracture enthalpy.

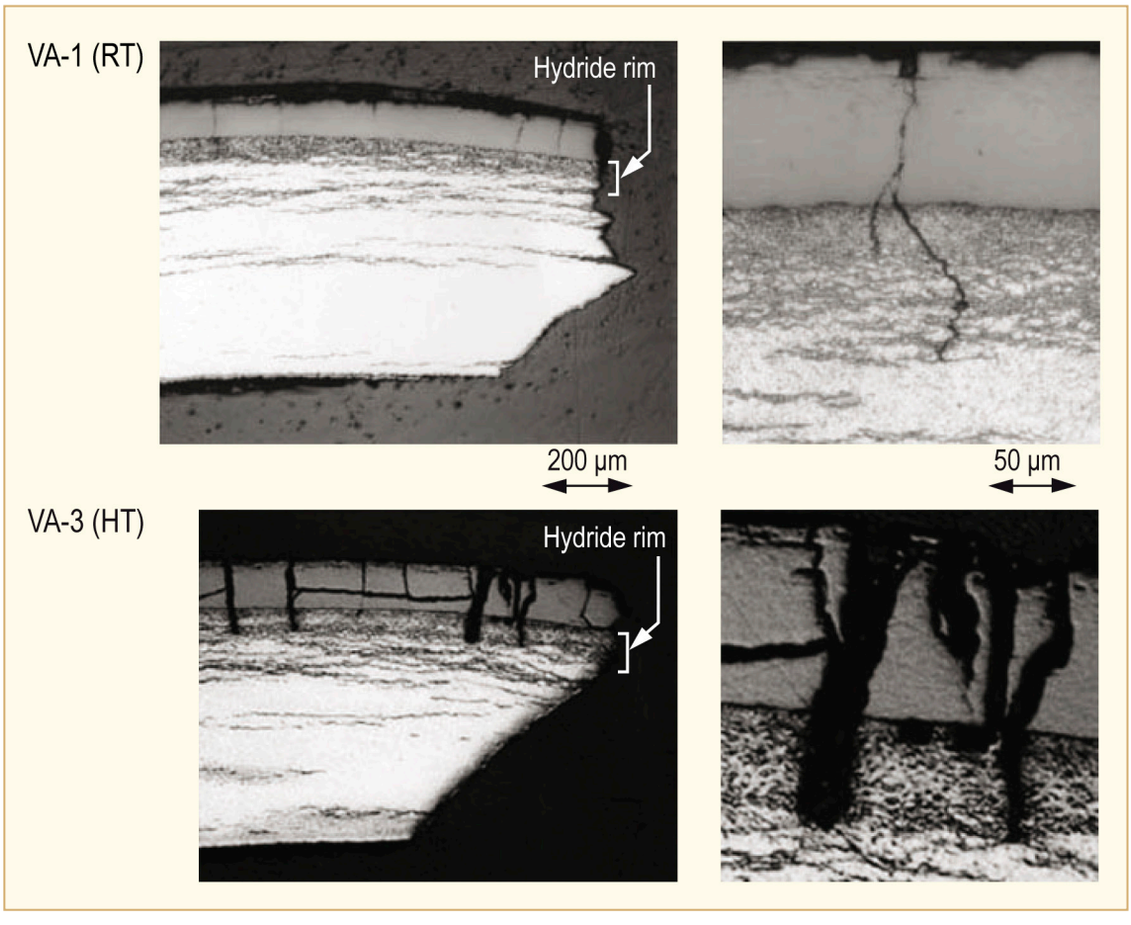

Figure 6-2: Metallographs of failed cladding in tests VA-1 and VA-3 [Sugiyama et al, 2009].

The second example in the same table is the two MDA sibling rods. Rod VA-2 was tested at RT and failed. Rod VA-4 was tested at HT and survived. Note that HT effect in this comparison is slightly confounded by the lower enthalpy increase of 109 cal/g (457 J/g) with HT rod (VA-4) as compared to 130 cal/g (546 J/g) with the RT rod (VA-2).

6.2 Pulse characteristics

6.2.1 Pulse characteristics (power increase rate, enthalpy increase, peak enthalpy, pulse width)

The transient power history under RIA, i.e. the power pulse imposed on the fuel, is generally characterized by two parameters: pulse width, and total energy deposition schematically shown in Figure 6-3. The pulse width is usually defined as the FWHM, whereas the total energy deposition is the time integral of fuel power, evaluated from beginning to end of the transient.

7 Results of energy and failure distribution calculations

Power pulses expected as a consequence of control rod ejection accidents in PWRs and control rod drop accidents in BWRs were discussed in section 2.2, where we concluded that the pulse width is a core-wide parameter, which for large reactivity insertions ($\Delta\rho > \beta$) is approximately proportional to the inverse of the prompt reactivity insertion $\Delta\rho$-β. The pulse amplitude, however, is a local property that falls off with increasing distance from the failed control rod, and it also depends on fuel burnup; see section 2.2.2.

To assess the consequences of an RIA, i.e. to estimate the number of failed fuel rods, it is necessary to first calculate the pulse amplitude and the resulting peak fuel enthalpy for each fuel rod.[27] The peak fuel enthalpy of each rod is then compared with relevant failure criteria, in which the state (burnup, internal gas overpressure, cladding corrosion, etc.) of the fuel rod is considered. A few studies of this kind are available in open literature. More specifically, state-of-the-art computational methods have been used to analyse postulated CREAs and CRDAs, and the distribution of energy and failed fuel rods have been calculated across the reactor core for these accident scenarios. An overview of reported studies on postulated CREAs is given in section 7.1, whereas section 7.2 summarizes analyses of CRDAs. All studies covered in these subsections relate to reactor cores with UO_2 fuel and were done with three-dimensional neutron kinetics codes, but large differences exist as to the postulated accident scenarios and reactivity additions. Moreover, the applied fuel rod failure criteria varied significantly between the reported studies.

7.1 Control rod ejection accidents in PWRs

Table 7-1 summarizes computational studies of postulated CREAs, in which calculated results on the distribution of energy and failed fuel rods across the reactor core are presented. All studies in Table 7-1 were done for end-of-cycle core conditions, and with two exceptions, they all pertain to CREAs that initiate from hot zero power reactor conditions.

Table 7-1: Summary of computational studies of postulated control rod ejection accidents, in which calculated distributions of energy and failed fuel rods are reported.

Core initial conditions	Reactivity insertion ($\Delta\rho/\beta$)	Peak enthalpy increase [$J(gUO_2)^{-1}$]	Fraction of failed rods [–]	Investigator [reference]
EOC HZP	1.89	247	0	Nakajima [2002]
EOC HZP	0.88	30	0	Dias et al. [1998]
EOC HZP	1.30	71	0	Dias et al. [1998]
EOC HZP	1.58	143	3.6×10^{-2}	Lee et al. [1995]
EOC HFP	0.15	83	9.0×10^{-3}	Lee et al. [1995]
EOC 30% of FP	1.58	112	9.0×10^{-3}	Gensler et al. [2015]

ANT International, 2016

For illustration, we will consider the study by Nakajima [2002]. This study was done for a typical four-loop PWR, in which the core consisted of 193 fuel assemblies of 17×17 design. The ejection of a fully inserted control rod was postulated at the end of a reactor operating cycle, while the core was held at hot zero power conditions. The reactivity worth of the ejected control rod, $\Delta\rho$, was increased from its realistic value of 6.0×10^{-3} to 8.7×10^{-3}, and penalizing assumptions were also made regarding

[27] Here, the peak fuel enthalpy refers to the peak value, with respect to time and axial position, of the radial average fuel enthalpy under the accident.

reactivity feedback effects, in order to increase the energy deposition to the fuel. The calculations were made with the EUREKA-JINS/S three-dimensional neutron kinetics code [Nakajima, 2002].

Figure 7-1 shows the position of the ejected control rod, together with the calculated distribution of energy in terms of peak fuel enthalpy. The highest enthalpy, 78 cal$(gUO_2)^{-1}$ or 327 J$(gUO_2)^{-1}$, is reached in a first cycle fuel assembly, neighbouring to the assembly from which the control rod is ejected. The fuel assembly loading pattern in the reactor core is shown to the right in Figure 7-1. The calculations show that first cycle fuel assemblies close to the ejected control rod position reach the highest fuel enthalpies, as a consequence of the comparatively high reactivity of low-burnup fuel. It is clear from Figure 7-1 that the calculated peak fuel enthalpy around the ejected control rod decreases rapidly, as the distance from the ejected rod increases. The enthalpy increases by more than 10 cal$(gUO_2)^{-1}$ in only 39 of the 193 fuel assemblies; the initial, pre-transient, fuel enthalpy was 19 cal$(gUO_2)^{-1}$ throughout the core.

The calculated peak fuel enthalpy increase of individual fuel rods is shown in Figure 7-2. The highest enthalpy increase is experienced by fuel rods in first cycle fuel assemblies, which have a fuel pellet average burnup below 20 MWd$(kgU)^{-1}$.

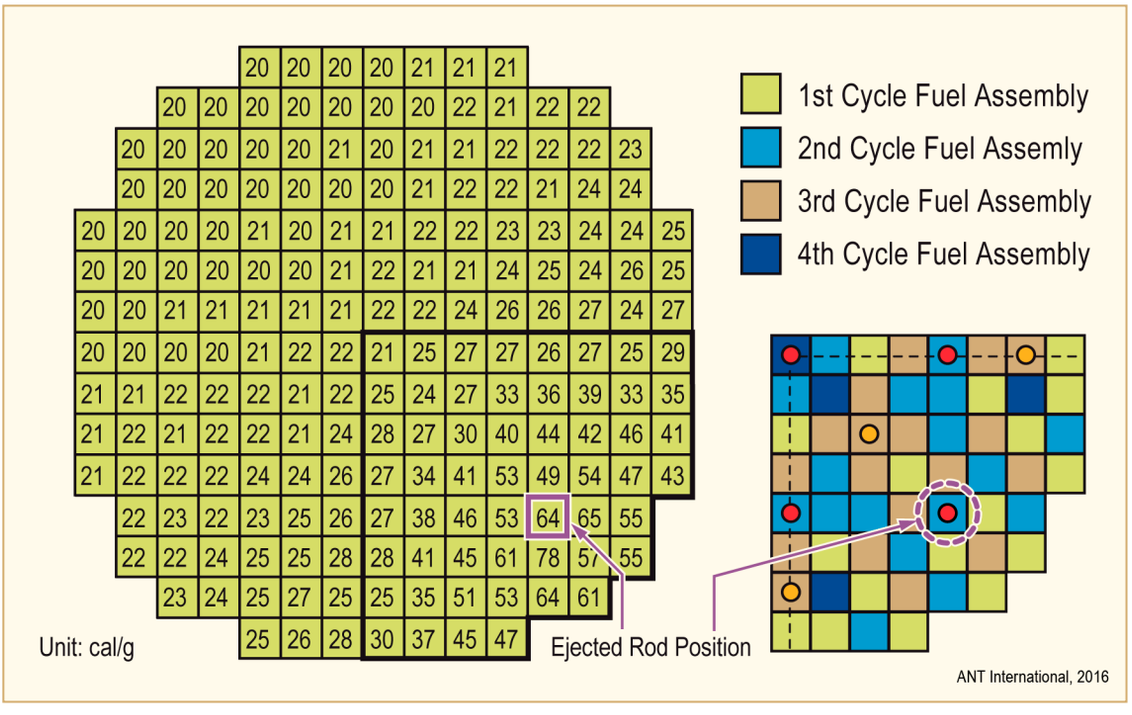

Figure 7-1: Calculated distribution of peak fuel pellet enthalpy, in units of cal$(gUO_2)^{-1}$, resulting from the postulated HZP CREA considered by Nakajima [2002].

For rods with higher burnup, the fuel enthalpy increase is typically below 45 cal$(gUO_2)^{-1}$, or 190 J$(gUO_2)^{-1}$. Since the calculated peak fuel enthalpies were well below all conceivable failure thresholds determined in pulse reactor tests, Nakajima concluded that all fuel rods in the core would survive the postulated accident [Nakajima, 2002].

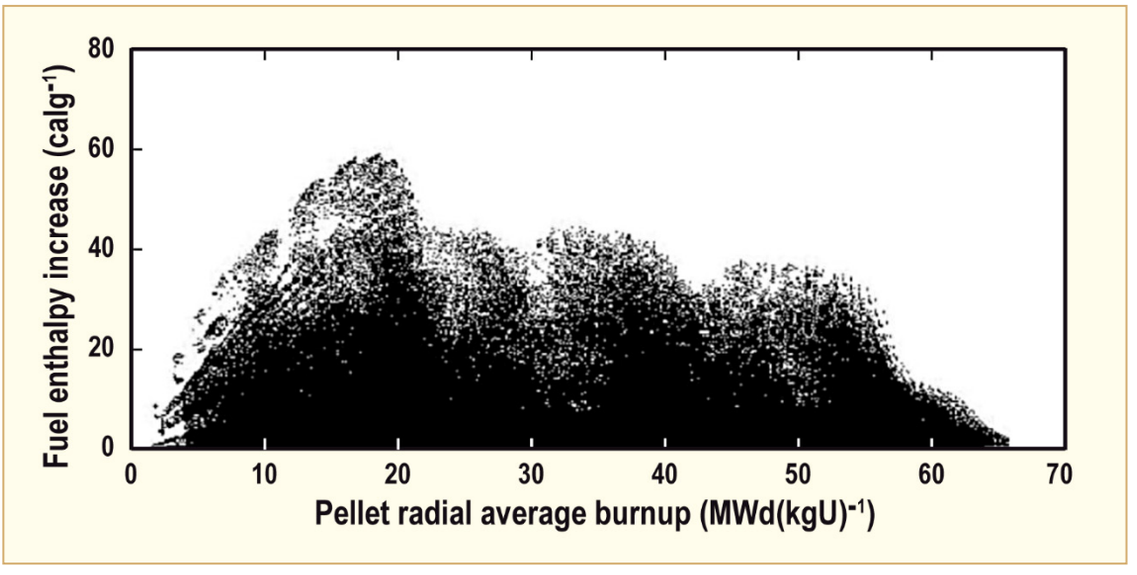

Figure 7-2: Scatter plot of calculated peak fuel enthalpy increase versus fuel pellet average burnup under the postulated HZP CREA considered by Nakajima [2002].

7.2 Control rod drop accidents in BWRs

Table 7-2 summarizes computational studies of postulated CRDAs, in which calculated results on the distribution of energy and failed fuel rods across the reactor core are presented. With one exception, the analyses in Table 7-2 were done for end-of-cycle core conditions. The studies pertain to CRDAs that initiate from either cold or hot zero power reactor conditions. For illustration, we will consider the analyses of CZP CRDAs by Nakajima [2002] and Heck et al. [1995].

Nakajima analysed a General Electric design BWR (BWR-5), in which the core comprised 764 fuel assemblies of 9×9 design. The postulated control rod drop occurred at the end of a reactor operating cycle under CZP conditions, meaning that the coolant was close to room temperature and atmospheric pressure, and the core power was negligible. The reactivity worth of the dropped control rod, $\Delta\rho$, was 1.3×10^{-2}, which is a conservative postulation and not a realistic value. The calculations were made with the EUREKA-JINS/S three-dimensional neutron kinetics code [Nakajima, 2002].

Figure 7-3 shows the position of the failed control rod, together with the calculated peak fuel enthalpy across the reactor core. The calculations show that the highest fuel enthalpy, 108 cal$(gUO_2)^{-1}$ or 452 J$(gUO_2)^{-1}$, is reached for a fuel rod in one of the four fuel assemblies that are adjacent to the dropped control rod. High enthalpies are reached also in the other three assemblies within this control cell. Outside the cell, however, the peak enthalpies are significantly lower.

8 Licensing/acceptance criteria for RIA

The main safety concerns in RIAs are loss of long-term core coolability and possible damage to the reactor pressure boundary and the core through pressure wave generation. Fuel failure, i.e. loss of clad tube integrity, is in itself generally not considered a safety concern (except in Germany), since fuel failures do not necessarily imply loss of coolable geometry or generation of harmful pressure waves. Nonetheless, RIA experiments and modelling have historically been focused on fuel rod failure, for several reasons:

- Fuel rod failure is a prerequisite for loss of coolable core geometry and pressure wave generation.
- The mechanisms for fuel rod failure are more easily studied, both experimentally and analytically, than those for gross core damage.
- Regulatory bodies require that the number of failed fuel rods in the core should be calculated in evaluations of radiological consequences to design basis RIA.

8.1 Current US regulations

Acceptance criteria for fuel behaviour under RIA were established by the United States Nuclear Regulatory Commission (USNRC) in the late seventies, based on results from early RIA simulation tests in pulse reactors [MacDonald et al, 1980]. These criteria, the details of which are given in RG-1.77, 1974 and [NUREG, 1981], have been used worldwide in their original or slightly modified forms, and they are therefore summarized below.

The *core coolability limit* of 280 cal/g-fuel (1172 J/g) was established based on the SPERT and TREAT experiments using zero or low burnup rods to investigate the failure consequences following a RIA event. The objective of a limit on the maximum radially averaged fuel enthalpy was to maintain coolable geometry and to eliminate the potential for fuel-coolant interaction and the generation of coolant pressure pulses that could damage the reactor core or pressure vessel. However, in establishing the 280 cal/g UO_2, the USNRC mistakenly expressed the RIA threshold in terms of radial average peak fuel enthalpy, while the SPERT and TREAT data were reported in terms of radial average total energy deposition. The radial average peak fuel enthalpy is less than the associated radial average total energy deposition due to fuel to coolant heat transfer during the transient and also since a significant part of the total energy is due to delayed fission. *The USNRC's failure limits of 280 cal/gUO_2 correspond to a peak radial average fuel enthalpy of 230 cal/gUO_2 (963 J/g).*

The *fuel rod failure threshold* related to *post-DNB failures (for unirradiated and/or low burnup fuel)* for RIA events is specified in [NUREG, 1981] and was established to meet the requirements of [NRC, 1990a] and [NRC, 1990b] GDC 19 as these relate to both on-site and off-site dose consequences. The fuel rod failure threshold for PWR and BWR applications is as follows:

- Regulatory Guide 1.77 states, "The number of fuel rods experiencing clad failure should be calculated and used to obtain the amount of contained fission product inventory released to the reactor coolant system". Clad failure should be assumed to occur when the calculated heat flux equals or exceeds the Departure from Nucleate Boiling Ratio (DNBR) for zero power, low power and full power RIA events in PWRs.
- The fuel rod failure threshold used in BWR's is defined in Standard Review Plan Sections 4.2 (II.A.2.f) and 15.4.9. Cladding failure should be assumed for rods that experience a maximum radially averaged fuel enthalpy greater than 170 cal/g for CCRDA, and events initiated from zero or low power. For rated power conditions, fuel rods that experience cladding dryout should be assumed to fail.

8.2 Modifications proposed by NRC for US requirements

In 2007, NRC published the interim RIA acceptance criteria, [NRC, 2007] based upon the available in-pile RIA test program data at that time.

In 2015, a revised memorandum [Clifford, 2015] was issued by NRC considering the results from the following reports: *This is an excellent source of information and it is recommended that the interested reader digest the information in this revised memorandum.*

1. OECD Nuclear Energy Agency State-of-the-art Report, "Nuclear Fuel Behaviour under RIA Conditions", 2010 [OECD, 2010].
2. EPRI Report 1021036, "Fuel Reliability Program: Proposed RIA Acceptance Criteria", December 2010 [EPRI, 2010].
3. Revised RIA transient fission gas release fractions [NRC, 2011].
4. PNNL Report 22549, "Pellet-Cladding Mechanical Interaction Failure Threshold for Reactivity Initiated Accidents for Pressurized Water Reactors and Boiling Water Reactors", June 2013 [PNNL, 2013].
5. Published results from NSRR Hot Capsule RIA Test VA3, VA4, RH2, BZ3, and LS2 (See [PNNL, 2013]).
6. JAEA published revised fuel enthalpy predictions for 43 previous NSRR test specimens [Udagawa et al, 2014].

In the following, the key results are provided.

8.2.1 Fuel cladding failure threshold

The number of fuel rod failures must not be underestimated to make sure that offsite and onsite radiological consequences criteria are satisfied. RIA fuel cladding failure mechanisms are the following:

1. Brittle Failures:
    a. High-temperature post-Departure from Nucleate Boiling (DNB) (film-boiling):
        i. oxygen-induced embrittlement and fragmentation.
    b. Pellet Cladding Mechanical Interaction (PCMI):
        i. Hydrogen-enhanced PCMI cladding failure.
2. Ductile Failure: High-temperature cladding creep (rod ballooning and burst).
3. Fuel Melt: Molten fuel-induced swelling PCMI cladding failure.

PCMI cladding failure (failure mechanisms #1b) is predicted to occur relatively early in the event prior to any significant increase in cladding temperature. *The clad ductility and specifically the embrittlement effect of hydrides is very much dependant on clad temperature*. Whereas, failure mechanisms #1a and #2 may occur in the later part of the event *when the RIA induced power transient has heated up the fuel cladding thereby reducing the tendency for PCMI failures*.

8.2.1.1 High temperature failure threshold (failure mechanisms #1a and #2)

The following revision to the RIA acceptance criteria and guidance is proposed:

- For zero power conditions, the high temperature cladding failure threshold is shown in Figure 8-1. This failure threshold considers both
  a. oxidation-induced embrittlement (failure mechanisms #1a)
  b. balloon and burst failure (failure mechanism #2).

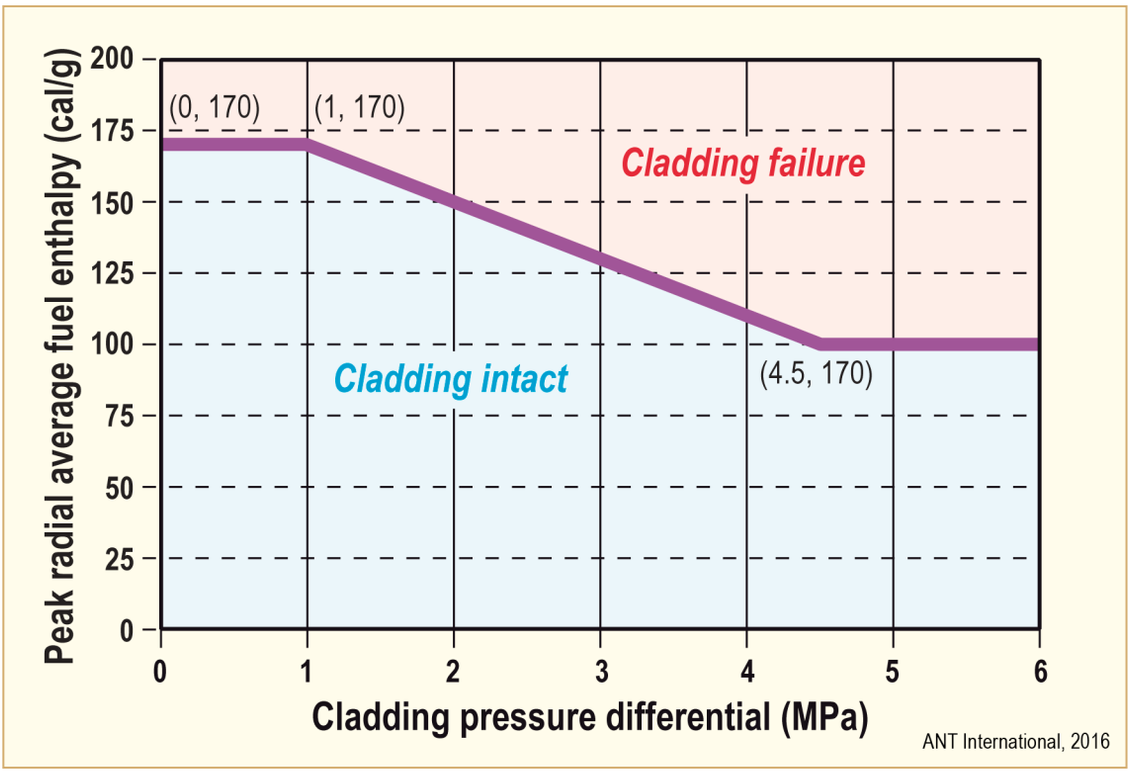

Figure 8-1: Revised High Temperature Cladding Failure Threshold, [Bales & Clifford, 2016].

- Predicted rod internal pressure must consider the impact of transient FGR on internal gas pressure.
- For intermediate and full power conditions, fuel cladding failure is presumed if local heat flux exceeds thermal design limits (e.g. DNBR and CPR).

The range of applicability is limited to the following conditions:

- All PWR and BWR UO_2 fuel rod designs with zirconium-based cladding, including barrier designs and fuel rods with both annular and solid pellets.
- BWR cold startup conditions up through PWR hot zero conditions.

8.2.1.2 Hydrogen-Enhanced PCMI Cladding Failure Technical Basis (failure mechanisms #1b)

The following considerations are tied to the cladding failure thresholds shown in Figure 8-2, Figure 8-4 and Figure 8-5:

- An approved alloy-specific cladding corrosion and hydrogen uptake model must be used to predict the initial, pre-RIA transient cladding hydrogen content.
- High confidence cladding hydrogen predictions for axial, radial, and circumferential variability and uncertainties should be used when implementing the PCMI failure thresholds.
- High confidence core physics predictions which account for biases and uncertainties should be used when implementing the PCMI failure thresholds.
- When applying the hydrogen dependent PCMI cladding failure curves, the cladding average (e.g., mid wall) temperature at the start of the transient should be used to define the amount of precipitated hydrogen in the cladding. Use of the Kearns solubility correlation is acceptable [Kearns, 1967].
- CZP and HZP calculations should encompass both (1) BOC conditions and (2) re-start following recent full power operation.
- Intermediate power levels up to HFP conditions should be evaluated to confirm power dependent core operating limits (e.g., control rod insertion limits, rod power peaking limits, axial and azimuthal power distribution limits).
- To calculate peak fuel enthalpy for CZP, zero fuel enthalpy is defined at 20°C (68°F).
- Cladding hydrogen contents and predicted fuel enthalpy change are expected to vary widely

  (1) between the fuel rods in the core and

  (2) axially along a given fuel rod.

- Since the PCMI failure threshold changes with cladding hydrogen content, the limiting scenario with respect to maximum number of failed rods may not be the highest worth control rod.
  - Applicants may need to survey a larger population of BWR blade drops and PWR ejected rods core locations and exposure points to identify the limiting scenario.

8.2.1.2.1 PWR Hot Operating Conditions

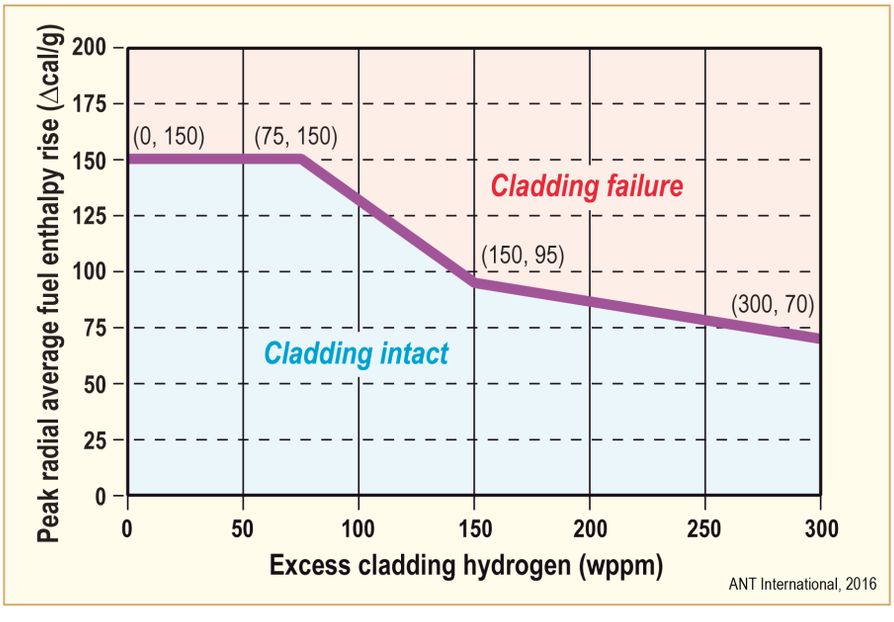

Figure 8-2: Revised PCMI cladding failure threshold, RXA cladding at PWR operating conditions, [Bales & Clifford, 2016]

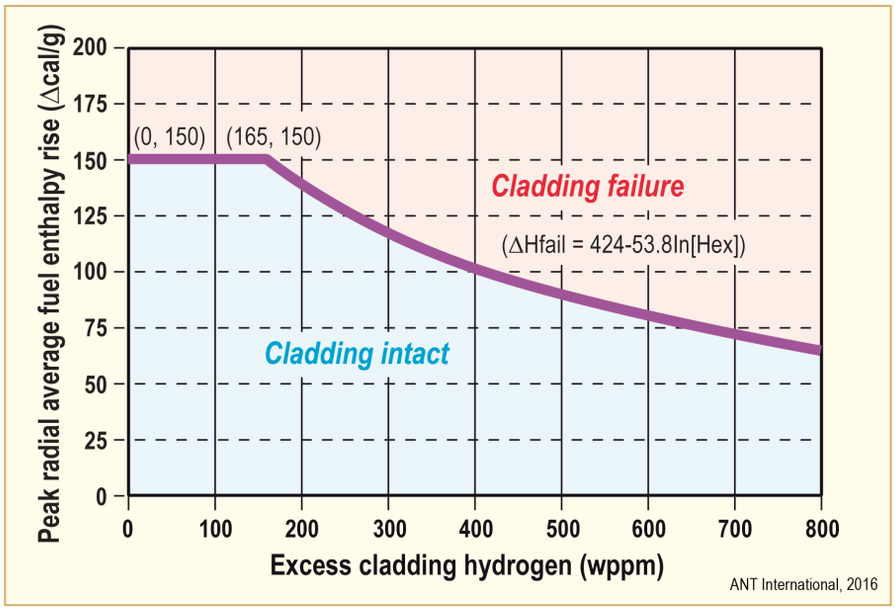

Figure 8-3: Revised PCMI cladding failure threshold, SRA cladding at PWR operating conditions, [Bales & Clifford, 2016]

8.2.1.2.2 BWR Cold Start-Up Conditions

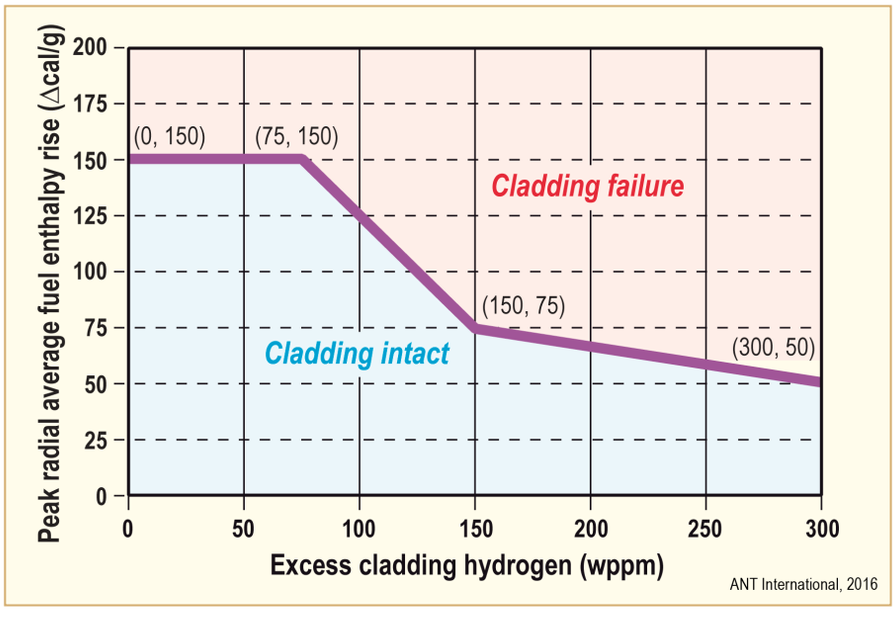

Figure 8-4: Revised PCMI cladding failure threshold, RXA cladding at BWR cold startup conditions, [Bales & Clifford, 2016]

Appendix C - (**information from ZIRAT18 STR on Mechanical Testing Vol. II**)

C.1 Mechanical testing techniques

Various scenarios for RIA events are described in earlier sections. Table C-1, Table C-2, and Table C-3 tabulate summaries. The cladding is generally presumed to experience two stages of mechanical loading which lead to plastic deformation and possible cladding rupture. The first phase is controlled by pellet clad mechanical interaction (PCMI) which is dominated by expansion of the fuel pellet against the inner cladding surface. Particularly at burnups higher than about 40 GWd/MT, the absence of a pellet-to-cladding gap and the presence of strong pellet-to-cladding chemical and mechanical bonding causes the cladding to be stretched in both the hoop (circumferential) and axial directions. The ratio of stresses in the two directions (σ_a/σ_h) is not precisely known; in the ideal case it might be close to 1 (i.e., 1/1) but in practice the ratio probably varies between 1 and 2. It is important to note that this is biaxial loading, not uniaxial loading as often occurs in other situations.

Table C-1: RIA mechanical loading conditions

Phase 1 – PCMI (pellet-cladding-mechanical interaction)
- Roughly equal biaxial (hoop +axial) stress - σ(a)/σ(h) = 1 ideally (or 1–2 in practice) - Strain rate high – 1–5 / s - Plane strain - Short duration – few tens of milliseconds
Phase 2 – clad ballooning
- High temperature and fission gas pressure
ANT International, 2016

Table C-2: RIA temperature conditions

PWR – control rod ejection
- Hot Zero Power (HZP) - 200°C< T<800°C - Average or optimum-- 400°C ??
BWR – control rod drop
- Cold Zero Power (CZP) - 30°C<T<300°C - Average or optimum– 100°C ??
ANT International, 2016

Table C-3: RIA mechanical testing techniques

Hoop to axial stress ratios
- 0/1 – uniaxial tension - 1/0 – open end burst test - 2/1 – closed end burst test - 1/1 – ideal for RIA stage 1
Specimens
- Many used for testing and analysis - Not all apply directly - Some axial, some hoop, some conventional from other applications
ANT International, 2016

Another key parameter is the ratio of strains in the two directions. An approximate conversion between the two is [Cazalis et al, 2005]:

Eq. C-1:
$$\frac{\varepsilon_{zz}}{\varepsilon_{\Theta\Theta}} = \frac{\left(\frac{2\sigma_{zz}}{\sigma_{\Theta\Theta}}\right) - 1}{2 - \frac{\sigma_{zz}}{\sigma_{\Theta\Theta}}}$$

This first phase is characterized by high heating rates in the cladding of about 10^3 K s^{-1} and high strain rates on the order of 1 s^{-1}. The cracks that form under RIA conditions are observed to form along the length of the cladding tube (axial direction) and to propagate primarily through the wall.

The heating pulse lasts a few tens of milliseconds. Many references to RIA scenarios exist. Three early ones are [de Betou et al, 2004; Desquines et al, 2004; Le Saux et al, 2007].

Cladding temperature is very important, particularly for high burnup fuel where hydride concentration can be in the 100–1000 ppm range. As discussed earlier, for PWRs the most severe accident occurs for a control rod ejection situation when the core is at hot zero power conditions [Nakajima et al, 2002]. Therefore the temperature starts at about 200°C (553K); during the millisecond pulse the cladding temperature rises to as high as 600°C (873K), [Desquines et al, 2004], or even higher (Figure C-1), [de Betou et al, 2004]. The optimum testing temperature is uncertain, but 400°C (673K) would seem to be a minimum. For BWRs the most severe condition is a control rod drop (CRDA) during cold zero power condition, [Nakajima et al, 2002], where the cladding starts at 30–100°C (303–373K). Increases in temperature are expected to be small, as evidenced by simulations conducted at the NSRR in Japan [Nakamura et al, 2000], [Nakamura et al, 2003], [Vitanza & Conde, 2004]. There it was shown, under conditions similar to a BWR CRDA, that cladding temperature during the pulse remained less than 100°C (373K).

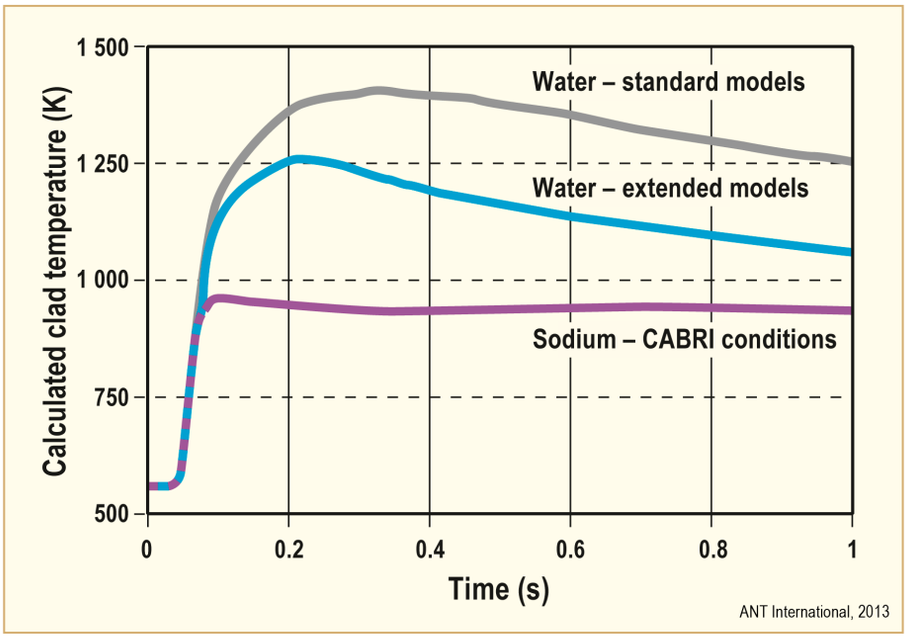

Figure C-1: Calculated clad temperatures during a PWR RIA with high burnup fuel (hot zero power), after [de Betou et al, 2004].

The second RIA phase occurs after the initial reactivity pulse decays. Due to the high temperature and possible fission gas release the internal pressure may be higher than the external pressure so the loading is creep-out pressure controlled. Clad temperature is thought to be as high as 800°C (1073K) [Desquines et al, 2004] approaching the temperature conditions of a LOCA. Also see Figure C-1. If the cladding has survived the first phase intact, clad ballooning and possible bursting could be expected. This stage has received little attention experimentally, as loss of ductility in phase I is the key potential issue.

C.1.1.1 Mechanical testing techniques

The most simple test to conduct is a uniaxial hoop tension one, where σ_h/σ_a = 1/0. However, this does not meet the biaxial stress criteria. Strain-to-failure is strongly influenced by biaxiality as illustrated in Figure C-2[Andersson & Wilson, 1979]. It is seen that the minimum fracture strain occurs when σh/σa is between 1 and 2. For reference, the uniaxial axial tensile test (σ_h/σ_a = 0/1) and the open end burst test (σ_h/σ_a = 1/0) bound the data, while a closed end burst test (σ_h/σ_a = 2/1) is in the minimum range. Note that (σ_h/σ_a = 1/1) is the “ideal” value for a RIA pulse.

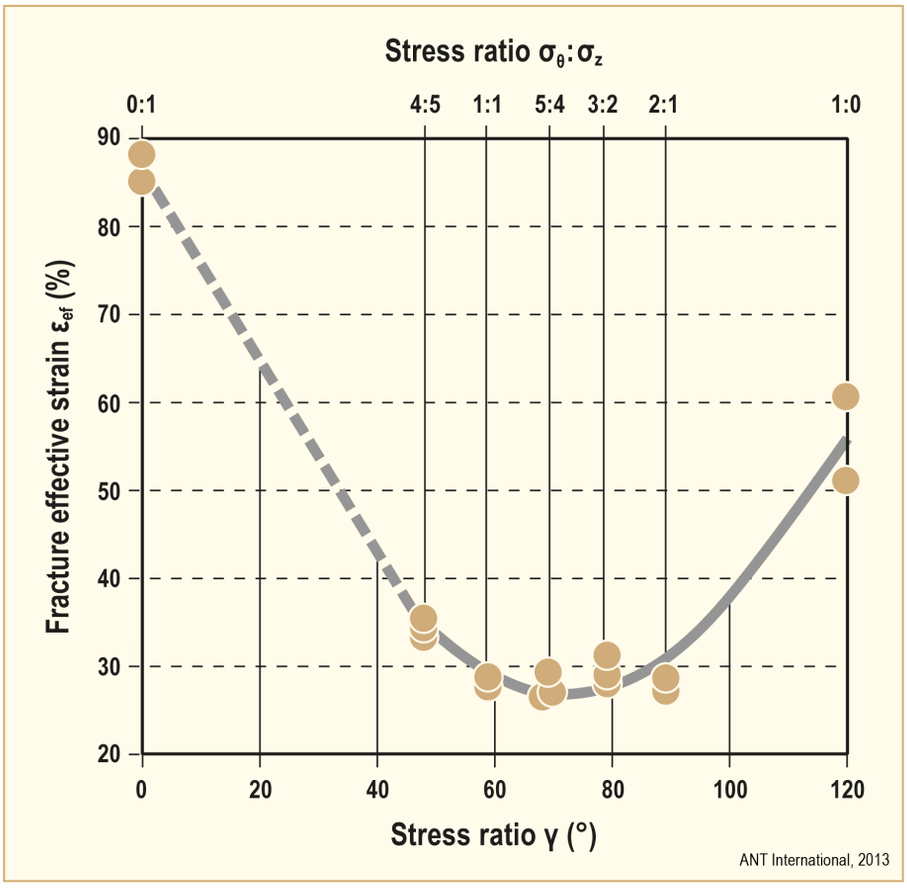

Figure C-2: Effect of stress ratio in testing on effective strain at fracture, after [Andersson & Wilson, 1979].

The correlation given in Figure C-2 was established for Zircaloy-4 having very low hydrogen concentrations, presumable <20 ppm. Other work, [Yunchang & Koss, 1985], determined that hydrides intensify the stress state effect.

Using equation C-1 and assuming plastic isotropy (and using the stress ratio as σ_z/σ_θ):

- Burst tests have a stress ratio of near 0.5 and a strain ratio close to zero; they can be considered as plane strain tests [Bernaudat & Pupiers, 2005].
- Hoop tensile tests have a zero stress ratio and a strain ratio close to –0.5.
- Equi-biaxial tension tests have stress and strain ratio of 1.

[Bernaudat & Pupier, 2005] used Figure C-4 to construct factors to correct failure strain from hoop tensile or burst (CEB) tests to conditions more similar to the "ideal" RIA case of equi-biaxial tension (Figure C-3)[31].

[31] Caution: Yunchang and Koss use longitudinal tension (rolling direction) and Bernaudat and Pupier use hoop (transverse) tests. They may not be equivalent.

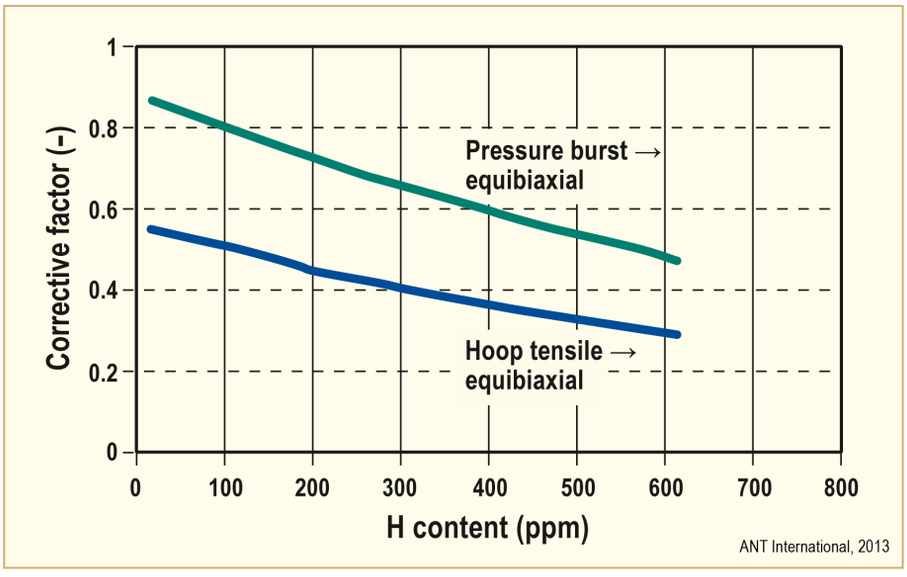

Figure C-3: Corrective factors to transpose the mechanical tests to the reactor situation, after [Bernaudat & Pupiers, 2005].

Figure C-4 shows that as hydrogen increases from 21 ppm to 615 ppm the differences between uniaxial tension (in this case, in the rolling direction rather than in the more interesting transverse direction), plane strain and equal biaxial tension increase.

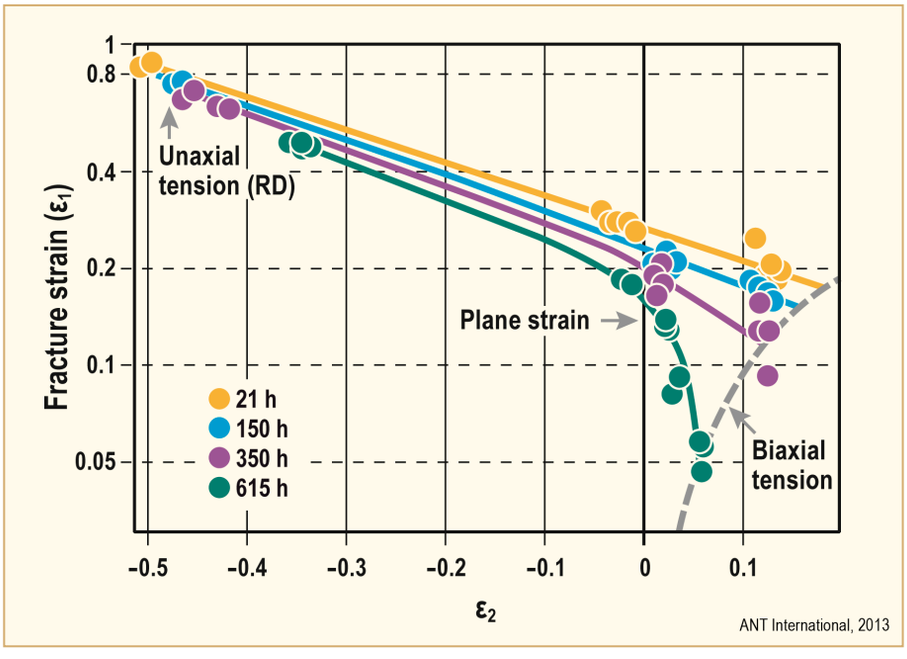

Figure C-4: A fracture limit diagram for Zircaloy-2 sheet with four levels of hydrogen. Tests conducted at room temperature. Principal strains in the plane of the sheet at fracture are given. ε_1 is the fracture strain, after [Yunchang & Koss, 1985].

In papers to be discussed later, [Carassou et al, 2009] and [Cazalis et al, 2005] give their estimates for the stress and strain states for various specimen configurations (note the inversion of the stress ratios as compared to Figure C-2), (Figure C-5), and for more clarity (Figure C-6).

References

Abe H., et al., *Development of advanced expansion due to compression (A-EDC) test method for safety evaluation of degraded nuclear fuel cladding materials,* Journal of Nuclear Science and Technology, 2015, 52(10): pp. 1232-1239.

Abe T., Nakae N., Kodato K. and Matsumoto M., *Failure behaviour of plutonium-uranium mixed oxide fuel under reactivity initiated accident condition,* Journal of Nuclear Materials, 1992, 188: pp. 154-161.

Adamson M. G., Aitken E. A. and Caputi R. W., *Experimental and thermodynamic evaluation of the melting behaviour of irradiated oxide fuels*, Journal of Nuclear Materials, 1985, 130: pp. 349-365.

Adamson R. B, Garzarolli F., Patterson C., Rudling P. and Strasser A., *ZIRAT14/IZNA9 Annual Report*, ANT International, Mölnlycke, Sweden, 2009.

Adamson R. B., Coleman K., Mahmood S. T. and Rudling P., *Mechanical testing of Zirconium alloys,* ZIRAT18/IZNA13 Special Topic Report, Vols. I and II, Advanced Nuclear Technology International, Mölnlycke, Sweden, 2013/2014.

Ade B., et al., *Safety and regulatory issues of the thorium fuel cycle,* Report ORNL/TM/2013/543 (NUREG/CR-7176), Oak Ridge National Laboratory, Oak Ridge, TN, USA, 2014.

Agee L. J., Dias A. F., Eisenhart L. D. and Engel R. E., *Realistic scoping study of reactivity insertion accidents for a typical PWR and BWR core*, Proc. CSNI specialist meeting on transient behaviour of high burnup fuel, pp. 291-304, Cadarache, France, September 12-14, 1995.

Amaya M., Sugiyama T., Nagase F. and Fuketa T., *Fission gas release in BWR fuel with a burnup of 56 GWd/t during simulated reactivity initiated accident (RIA) condition,* Journal of Nuclear Science and Technology, 2008, 45(5): pp. 423-431.

Amaya M., Udagawa Y., Narukawa T., Mihara T. and Sugiyama T, *Behavior of high burnup advanced fuels for LWR during design-basis accidents*, 2015. In: TopFuel-2015*,* Zürich, Switzerland: European Nuclear Society, pp. 10-18, September 13-17, 2015.

Amaya M., et al. *Behavior of high-burnup advanced LWR fuels under accident conditions*, 2016. In: TopFuel 2016*,* Boise, ID, USA: American Nuclear Society, pp. 53-62, September 11-15, 2016.

Andersson T. and Wilson A, *Ductility of Zircaloy canning tubes in relation to stress ratio in biaxial testing*. In: Zirconium in the nuclear industry; 4th international symposium: J.H. Schemel and T.P. Papazoglou, Eds., American Society for Testing and Materials, ASTM STP-681, pp. 60-71, 1979.

Arséne S. and Bai J. B., *A new approach to measuring transverse properties of structural tubing by a ring tes*t, Journal of Testing and Evaluation (JTEVA), 1996, 24(6): pp. 386-391.

Asmolov V. and Yegorova L., *The Russian RIA research program: Motivation, definition, execution and results,* Nuclear Safety, 1996, 37(4): pp. 343-371.

Azuma M., Taniguchi A., Hotta A. and Ohta T., *Assessment on integrity of BWR internals against impact load by water hammer under conditions of reactivity initiated accidents,* Nuclear Technology, 2005, 149: pp. 243-252.

Bales M. and Clifford P, *Proposed Changes in Regulation for LOCAand RIA in the US*, Fuel Safety Research Meeting, Mito, Japan, October 18–19, 2016.

Balourdet M. and Bernaudat C., *Tensile properties of Zircaloy-4 cladding submitted to fast transient loading*, 1995. In: CSNI specialist meeting on transient behaviour of high burnup fuel, Cadarache, France: OECD Nuclear Energy Agency, NEA/CSNI/R(95)22, pp. 417-431, September 12-14, 1995.

Balourdet M., et al. *The PROMETRA programme: Assessment of mechanical properties of Zircaloy-4 fuel cladding during an RIA*, 1999. In: 15th international conference on structural mechanics in reactor technology (SMiRT-15), Seoul, Korea, Vol II, pp. 485-492, August 15-20, 1999.

Bates D.W., et al. *Influence of specimen design on the deformation and failure of Zircaloy cladding*. In: ANS topical meeting on light water reactor fuel performance, Park City, Utah, USA: American Nuclear Society, pp. 296-305, April 10-13, 2000.

Bernaudat C. and Pupier P., *A new analytical approach to study the rod ejection accident in PWRs*, Water Reactor Fuel Performance Meeting, Japan, October, 2005.

Berthoud G., *Vapor explosions,* Annular Review of Fluid Mechanics, 2000, 32: pp. 573-611.

Bessiron V., *The PATRICIA program on clad to coolant heat transfer during reactivity initiated accidents*. In: Tenth international topical meeting on nuclear reactor thermal hydraulics (NURETH-10), Seoul, Korea, October 5-9, 2003.

Bessiron V., *Clad-to-coolant heat transfer during a RIA transient: Analysis of the PATRICIA experiments, modelling and applications*. In: Fuel safety research meeting, Tokyo, Japan, March 1-2, 2004.

Bessiron V., *Modelling of clad to coolant heat transfer for RIA applications,* Journal of Nuclear Science and Technology, 2007, 44(2): pp. 211-221.

Bodansky D., *Nuclear Energy: Principles, practices and prospects*. 2nd ed., New York: Springer AIP Press, 2004.

Bogdanov V.N., et al. *Irradiating complex on BIGR reactor for simulation accidents of RIA type*. In: Seventh international conference on nuclear criticality and safety, Tokai, Japan: Japan Atomic Energy Research Institute, pp. 770-772, October 20-24, 2003.

Bourguignon D., *The new CABRI water loop: Detailed description of the new water loop and of the specific new zircaloy in-core experimental cell*. In: 10th Meeting of the International Group on Research Reactors, Gaithersburg, MD, USA, September 12-16, 2005.

Carbajo J., Yoder G., Popovb S. and Ivanov V., *A review of the thermophysical properties of MOX and UO_2 fuels* Journal of Nuclear Materials, 2001, 299: pp. 181-198.

Carassou S. et al, *Ductility and Failure Behaviour of both Unirradiated and Irradiated Zircaloy-4 Cladding Using Plane Strain Tensile Specimens*, OECD/NEA Workshop, Nuclear Fuel Behaviour during RIA, Paris, Sept. 2009.

Carey V. P., *Liquid-vapor phase-change phenomena: An introduction to the thermophysics of vaporization and condensation processes in heat transfer equipment*, 2nd ed., Taylor & Francis, Washington, USA, 2007.

Carmack W.J., et al., *Inert matrix fuel neutronic, thermal-hydraulic, and transient behavior in a light water reactor*. Journal of Nuclear Materials, 2006, 352(1-3): pp. 276-284.

Cazalis B., et al. *The PROMETRA program: A reliable material database for highly irradiated Zircaloy-4, ZIRLO and M5 fuel claddings*. In: 18th international conference on structural mechanics in reactor technology (SMiRT-18), Beijing, China, pp. 383-393, August 7-12, 2005.

Cazalis B., et al., *The PROMETRA program: Fuel cladding mechanical behavior under high strain rate,* Nuclear Technology, 2007, 157: pp. 215-229.

Cazalis B. and Georgenthum V., *MOX fuel behaviour under reactivity initiated acciden*. In: TopFuel-2012 Manchester, UK: European Nuclear Society, pp. 176-182, September 2-6, 2012.

Cazalis B., et al., *The plane strain tests in the PROMETRA program,* Journal of Nuclear Materials, 2016a, 472: pp. 127-142.

Cazalis B., et al. *The PROMETRA program: Plane strain tests on fresh and highly irradiated Zircaloy-4, ZIRLO and M5 fuel claddings*, 2016. In: TopFuel 2016, Boise, ID, USA: American Nuclear Society, pp. 879-888, September 11-15, 2016b.

Clifford P. M., *Technical and Regulatory Basis for the Reactivity-Initiated Accident Acceptance Criteria and Guidance*, Revision 1, March 16, 2015.

Christensen J. A., Allio R. J. and Biancheria A., *Melting point of irradiated uranium dioxide*, Transactions of the American Nuclear Society, 1964, 7(2): pp. 390-391.

Chu H.C., et al., *Effect of radial hydrides on the axial and hoop mechanical properties of Zircaloy-4 cladding,* Journal of Nuclear Materials, 2007, 362: pp. 93-103.

Chung H.M. and Kassner T.F., *Cladding metallurgy and fracture behavior during reactivity-initiated accidents at high burnup,* Nuclear Engineering and Design, 1998, 186: pp. 411-427.

Clifford P. M., *Technical and Regulatory Basis for the Reactivity-Initiated Accident Acceptance Criteria and Guidance*, Revision 1, March 16, 2015.

Cook B.A., et al., *Reactivity initiated accident test series, Test RIA 1-2 fuel behavior report,* Report NUREG/CR-1842, US Nuclear Regulatory Commission, Washington DC, USA, 1981.

Cook B.A. and Martinson Z.R., *Reactivity initiated accident test series, test RIA 1-4 fuel behavior report,* Report NUREG/CR-3938, US Nuclear Regulatory Commission, Washington DC, USA, 1984.

Corradini M.L., et al., *Vapor explosions in light water reactors: A review of theory and modelling,* Progress in Nuclear Energy, 1988, 22(1): pp. 1-117.

Da Cruz D.F. and Mittag S., *Safety issues on the deployment of thorium fuel in pressurized water reactors*. In: GLOBAL 2011: Tenth International Conference: Toward and over the Fukushima Daiichi Accident, Chiba, Japan: Atomic Energy Society of Japan, December 11-16, 2011.

Dagbjartsson S.J., et al., *Axial gas flow in irradiated PWR fuel rods,* TREE-NUREG-1158, US Nuclear Regulatory Commission, Washington DC, USA, 1977.

Daum R.S., et al., *Mechanical property testing of irradiated Zircaloy cladding under reactor transient conditions*. In: Small specimen test techniques: Fourth volume: M.A. Sokolov, J.D. Landes, and G.E. Lucas, Editors, American Society for Testing and Materials, ASTM STP-1418, 2002a.

Daum R.S., et al., *On the embrittlement of Zircaloy-4 under RIA-relevant conditions*. In: Zirconium in the nuclear industry; 13th international symposium: G.P. Moan and P. Rudling, Editors, American Society for Testing and Materials, ASTM STP-1423, pp. 702-719, 2002b.

Daum R.S., et al., *Radial-hydride embrittlement of high-burnup Zircaloy-4 fuel cladding,* Journal of Nuclear Science and Technology, 2006, 43(9): pp. 1054-1067.

de Betou J., et al., *Assessment of burnup-dependent fuel rod failure threshold under reactivity-initiated accidents in light water reactors*. In: 2004 International meeting on light water reactor fuel performance, Orlando, FL, USA: American Nuclear Society, September 19-22, 2004.

Desquines J., Cazalis B., Bernaudat C., Poussard C., Averty X. and Yvon P., *Mechanical Properties of Zircaloy-4 PWR Fuel Cladding with Burnup of 54-64- GWD/MT and Implications for RIA Behaviour,* 14th Int. Symposium on Zirconium in the Nuclear Industry, Stockholm, Sweden, ASTM STP 1467, June, 2004.

Desquines J., et al., *Mechanical properties of Zircaloy-4 PWR fuel cladding with burnup 54-64 MWd/kgU and implications for RIA behavior,* Journal of ASTM International, 2005, 2(6).

Desquines J., et al., *The issue of stress state during mechanical tests to assess cladding performance during a reactivity-initiated accident (RIA),* Journal of Nuclear Materials, 2011, 412: pp. 250-267.

Diamond D. J., Bromely B. P. and Aronson A., *Pulse width during a PWR rod ejection accident*, Proc: 29th Nuclear Safety Conference, Washington, DC, USA, October, 2001.

Diamond D.J., et al., *Studies of the rod ejection accident in a PWR,* Technical report W-6382, Brookhaven National Laboratory, Upton, NY, USA, 2002.

Nomenclature

The symbols and abbreviations used in this report are listed below, together with a brief explanation to the notation. The symbols used conform as far as possible to prevalent nomenclature in international literature. Throughout the text, all mathematical symbols are printed in italic. The international system of units (SI) is applied.

Latin symbols:

c_f	Fuel specific heat capacity	[$J(gK)^{-1}$]
d_{32}	Mean diameter (volume-to-surface diameter)	[m]
E_{tot}	Total energy deposited to the fuel	[$J(gUO_2)^{-1}$]
h_f	Fuel pellet specific enthalpy (radial average)	[Jg^{-1}]
k_{eff}	Effective neutron multiplication factor	[-]
k_∞	Infinite lattice multiplication factor	[-]
L_o	Test specimen gauge length	[m]
P_{max}	Power pulse amplitude	[$W(gUO_2)^{-1}$]
t	Time	[s]
T	Temperature	[K]
T_0	Reference temperature, at which h_f=0. Here, T_0=273 K	[K]
T_f	Fuel temperature	[K]
T_m	Moderator temperature	[K]
T_s	Solidus (melting) temperature	[K]
W_o	Test specimen gauge section with	[m]

Greek symbols:

α_m	Moderator void volume fraction	[-]
β	Effective delayed neutron fraction	[-]
ΔP	Fuel rod internal gas overpressure	[Pa]
$\varepsilon_{\theta\theta}$	Hoop (circumferential) strain	[-]
ε_{zz}	Axial (longitudinal) strain	[-]
Λ	Effective neutron lifetime	[s]
ρ	Reactivity	[-]
σ	Uniaxial or effective stress	[Pa]
$\sigma_{\theta\theta}$	Hoop (circumferential) stress	[Pa]
σ_{zz}	Axial (longitudinal) stress	[Pa]
τ	Pulse width (Full width at half maximum - FWHM)	[s]

List of Abbreviations

ACPR	Annular Core Pulse Reactor
AECL	Atomic Energy of Canada Limited
AISI	American Iron and Steel Institute
ANL	Argonne National Laboratory (USA)
ANSI	American National Standards Institute
ANT	Advanced Nuclear Technology
AOA	Axial Offset Anomaly
AOO	Anticipated Operating Occurrence
AREVA	French Equipment Manufacturer
ASEA	Allmänna Svenska Elektriska Aktiebolaget (General Swedish Electrical Limited Company)
ASME	American Society of Mechanical Engineers
ATF	Accident Tolerant Fuel
ATR	Advanced Thermal Reactor
AUC	Ammonium uranocarbonate
B&W	Babcock & Willcox
BA	Burnable Absorber
BCC	Body Centred Cubic
BIGR	Fast Impulse Graphite Reactor (Russia)
BNFL	British Nuclear Fuels Limited
BOC	Beginning of Cycle
BOP	Balance of Plant
BR3	Belgian Reactor 3 (Belgium)
BWR	Boiling Water Reactor
CANDU	Canadian Deuterium Uranium
CASL	Consortium for Advanced Simulation of LWRs
CE	Combustion Engineering
CEA	Commissariat à l´Energie Atomique et aux Énergies Alternatives (French atomic energy commission)
CILC	CRUD Induced Localized Corrosion
CIP	CABRI International Program
CIPS	CRUD Induced Power Shift
CP	Corrosion Product
CR	Control Rod
CRDA	Control Rod Drop Accident
CREA	Control Rod Ejection Accident
CRUD	Chalk River Unidentified Deposits
CSED	Critical Strain Energy Density
CVCS	Chemical and Volume Control System
CWSR	Cold Work and Stress Relieved
CZP	Cold Zero Power
DNB	Departure from Nuclear Boiling
E110	Cladding material used in VVER fuel rods (Zr-1.0Nb by wt%)
ECBE	Effective Control Blade Exposure
EDC	Expansion Due to Compression
EDF	Electricité de France
EFID	Effective Full Insertion Days
ELS	Extra-Low Sn
EOC	End Of Cycle
EPRI	Electric Power Research Institute (USA)
ESSC	Enhanced Spacer Shadow Corrosion
ETR	Engineering Test Reactor (USA)
FA	Fuel Assembly
FCI	Fuel-Coolant Interaction
FGR	Fission Gas Release
FP	Fission Product
FRED	Fuel Reliability Data Base

Unit conversion

TEMPERATURE		
°C + 273.15 = K	°C × 1.8 + 32 = °F	
T(K)	T(°C)	T(°F)
273	**0**	32
289	16	61
298	25	77
373	**100**	212
473	**200**	392
573	**300**	572
633	360	680
673	**400**	752
773	**500**	932
783	510	950
793	520	968
823	550	1022
833	560	1040
873	**600**	1112
878	605	1121
893	620	1148
923	650	1202
973	**700**	1292
1023	750	1382
1053	780	1436
1073	**800**	1472
1136	863	1585
1143	870	1598
1173	**900**	1652
1273	**1000**	1832
1343	1070	1958
1478	1204	**2200**

Radioactivity	
1 Sv	= 100 Rem
1 Ci	= 3.7×10^{10} Bq = 37 GBq
1 Bq	= 1 s^{-1}

MASS	
kg	lbs
0.454	**1**
1	2.20

DISTANCE	
x (µm)	x (mils)
0.6	0.02
1	0.04
5	0.20
10	0.39
20	0.79
25	0.98
25.4	**1.00**
100	3.94

PRESSURE		
bar	MPa	psi
1	0.1	14
10	**1**	142
70	7	995
70.4	7.04	**1000**
100	10	1421
130	13	1847
155	15.5	2203
704	70.4	**10000**
1000	100	14211

STRESS INTENSITY FACTOR	
MPa√m	ksi√inch
0.91	**1**
1	1.10